Neuromodulatory Circuits of Feeding Drive

B.S – M.S Thesis

Akash G

20091107

Under the guidance of

Dr. Aurnab Ghose

Biology Division, IISER Pune

Certificate

This is to certify that this dissertation entitled “Neuromodulatory circuits of feeding drive” towards the partial fulfillment of the BS-MS dual degree program at the Indian Institute of Science Education and Research, Pune represents original research carried out by Akash G at IISER Pune under the supervision of Dr. Aurnab Ghose, Assistant Professor, Biology Division, IISER Pune during the academic year 2013-2014.

Dr. Aurnab Ghose

Assistant Professor

Biology Division, IISER Pune

Declaration

I hereby declare that the matter embodied in the report entitled “Neuromodulatory circuits of feeding drive” are the results of the investigations carried out by me at the Department of Biology, IISER Pune, under the supervision of Dr. Aurnab Ghose and the same has not been submitted elsewhere for any other degree.

Akash G

B.S – M.S Dual Degree Student

IISER Pune

Abstract

Neural circuits of innate behaviors which are necessary for survival are redundant and hardwired as they are shaped by selective pressure. However, functional organization of these circuits is poorly understood. Here we focus on Cocaine- and Amphetamine- Regulated Transcript (CART) neural circuitry in regulation of feeding drive. Using gene specific, *in situ* hybridization, we have mapped the expression pattern of the four CART genes in the adult zebrafish brain. CART 2 and 4 were expressed in many regions involved in sensory processing, neuroendocrine regulation, and motor control while CART 1 and 3 showed restricted expression in nucleus of the medial longitudinal fasciculus (NMLF) and in the entopeduncular nucleus (EN) respectively. We have identified CART expressing neuronal groups which respond to changes in energy levels. In hypothalamus, upon starvation, CART 2 expression in the nucleus recessus lateralis (NRL) was completely abolished and CART 4 expression was reduced in the nucleus lateralis tuberis (NLT) suggesting their important role in energy homeostasis. EN in telencephalon emerges as a novel non-hypothalamic nucleus involved in energy homoeostasis as CART 2 expression was significantly reduced upon starvation. These nuclei could serve as an entry point for circuit specific investigation of feeding behavior. To that end we have optimized a high throughput behavioral assay to quantify feeding behavior in zebrafish larvae using fluorescently labeled paramecia. Energy homoeostasis may modulate olfactory sensitivity towards food related odorants. We have optimized electro-olfactogram (EOG) for zebrafish and our preliminary data suggests an increased olfactory sensitivity in starved fish.

Table of Contents

List of Figures

Acknowledgements

Working on this project was an exciting and intellectually enriching experience. I express my deep gratitude to Dr. Aurnab Ghose and Dr. N.K. Subhedar for their valuable, inspiring, encouraging guidance and providing me with a great scientific atmosphere, where I could think independently and take bold steps. Apart from research, I have learnt a lot on how and why to pursue research, how to get excited about finer things in life. These molded my overall scientific development for which I am heavily indebted to them.

I am thankful to Dr. Raghav Rajan for providing me with materials and guiding me throughout EOG setup development. I have learnt a lot of engineering techniques, electronics and methods of improvisation for which I am grateful to him.

I would like to thank Tarun Kaniganti for helping me with my experiments and all my lab members Ajinkya, Debia, Kaweri, Neeraj, Aditi, Devika, Ketki, Abhishek R, Prashant, Abhishek S, Ketakee, Sampada and Tanushree for assisting, teaching, and encouraging me all through the project and for maintaining a fun atmosphere in the lab.

I thank my friends, and family for showing faith and providing confidence during my entire IISER life.

I thank IISER Pune for providing me this wonderful opportunity to grow and develop both scientifically and personally.

Abbreviations

AC anterior commissure
BC brachium conjunctivum
C central canal
CART cocaine- and amphetamine-regulated transcript
CB cerebellum
CC corpus cerebella
CP central posterior thalamic nucleus
D dorsal telencephalic area
Dc central zone of the dorsal telencephalic area
Dd dorsal zone of the dorsal telencephalic area
DH dorsal horn
DIL diffuse nucleus of the inferior hypothalamic lobe
DiV diencephalic ventricle
Dl lateral zone of the dorsal telencephalic area
Dm medial zone of the dorsal telencephalic area
Dp posterior zone of the dorsal telencephalic area
DTN dorsal tegmental nucleus
EG eminentia granularis
EN entopeduncular nucleus
EW Edinger-Westphal nucleus
Fd funiculus dorsalis
Fld funiculus lateralis (pars dorsalis)
Flv funiculus lateralis (pars ventralis)
Fv funiculus ventralis
GL glomerular layer of the olfactory bulb
Ha habenula
HaC habenular commisure
HC horizontal commissure
Hc caudal zone of periventricular hypothalamus
Hv ventral zone of periventricular hypothalamus
Hy hypophysis / pituitary gland
ICL internal cell layer of olfactory bulb
IMRF intermediate reticular formation
IO inferior olive
IRF inferior reticular formation
LCa lobus caudalis cerebelli
LLF lateral longitudinal fascicle
LRN lateral reticular nucleus
LVII lobus facialis
LX lobus vagus
MLF medial longitudinal fascicle
MO medulla oblongata
NLT nucleus lateralis tuberis
NMLF nucleus of the medial longitudinal fascicle
NPY Neuropeptide Y
NRL nucleus recessus lateralis
OB olfactory bulb
OC optic chiasma
OTr optic tract
PC posterior commissure
PG preglomerular nucleus
PGZ periventricular gray zone of optic tectum
PM magnocellular preoptic nucleus
POA preoptic area
poc post optic commissure
PPa anterior part of parvocellular preoptic nucleus
PPp posterior part of the parvocellular preoptic nucleus
PTN posterior tuberal nucleus
RV rhombencephalic ventricle
SAC stratum album central
SC spinal cord
SCN suprachiasmatic nucleus
SFGS stratum fibrosum et griseum superficiale
SM stratum marginale
SO stratum opticum
SR superior raphe
SRF superior reticular formation
T telencephalon
TeO optic tectum
TeV telencephalic ventricle
TL torus longitudinalis
TLa torus lateralis
TPp periventricular nucleus of posterior tuberculum
TS torus semicircularis
VAO ventral accessory optic nucleus
Vc central nucleus of the ventral telencephalic area
Vd dorsal nucleus of the ventral telencephalic area
VH ventral horn
Vl lateral nucleus of the ventral telencephalic area
VM ventromedial thalamic nucleus
Vs supracommissural nucleus of the ventral telencephalic area
Vv ventral nucleus of the ventral telencephalic area

Chapter 1

Introduction

The behavioral repertoire of different organisms is very diverse ranging from simple motor outputs such as wriggling the tail to complex decision making. Many of these behaviors which are either innate or learnt arise due to the internal state of the body. For example, the innate drives to forage and consume food, search and drink water, find and attract a mate are some behaviors which are energetically costly but are necessary for survival and reproduction. The organism has to choose a particular set of behaviors from a wide range of behaviors to minimize the energy cost and this is done by some yet unknown mechanism of computing external environmental states and internal states of the body. How does an organism decide when to consume food and when not to, when to sleep and when to stay active?

Such behaviors are intriguing, and raise many interesting questions. How are different internal physiological states of the body sensed in the brain? Many of the internal physiological states vary slowly. How is this gradual change processed to produce a behavioral switch? What are the computations involved? How this computation is effected in motor outputs? To answer these questions one need to understand the underlying neural circuits. Such neural circuitry may consist of interoceptive neurons which sense internal state, neurons which integrate information from different neuronal populations, neurons which code for switching behaviors, neurons which select actions and downstream neurons which execute the behavior.

Feeding Drive

The ‘feeding drive’ is a result of different energy homeostasis mechanisms which regulate behaviors such as foraging, risk assessment, fear, sensory processing and food intake. Consuming food to counteract physiological deficit is one of the basic innate purposive behavior which is necessary for survival. Neural circuits underlying such complex behaviors are expected to be hardwired, redundant and under strong

developmental control. We aim to study the neural processes and computations involved in the neural circuits regulating the feeding drive.

Strategy to study neural processes influencing feeding behavior

The key steps in understanding the neural processes regulating feeding behavior are 1. Ability to quantify feeding behavior. 2. Identify molecularly defined interoceptive neuronal populations which sense internal states of the body. 3. Identify other neurons which define the behavior by axonal tracing using the interoceptors as starting point. 4. Test causality, necessity and sufficiency of these neurons by manipulating their activity and studying behavioral changes 5. Study the contribution of these neurons and axons with their synaptic partners and understand the computations involved. We plan to investigate the neural circuits involved in feeding drive using this reverse engineering approach.

In this study, we focus on Cocaine- and Amphetamine- Regulated Transcript, a neuropeptide known to have important role in energy homoeostasis. We have identified genetically defined CART neuronal populations which respond to changes in energy levels. We adopt a strategy to use these neurons as starting point, figure out the axonal projections and elucidate the neural circuitry regulating the feeding drive. We also explore an additional dimension of feeding drive which is modulation of sensory sensitivity in relation to energy status. Change in sensory sensitivity affects behaviors such as foraging, risk assessment, olfaction and palatability, thus affecting feeding drive.

Cocaine- and Amphetamine- regulated transcript

Cocaine- and Amphetamine –regulated transcript (CART) is a neuropeptide and a neuromodulator which is widely distributed across vertebrate phyla. CART initially thought to be up regulated on administration of cocaine or amphetamine (Douglass et al., 1995), was later found to have a role in diverse functions such as in addiction (Hubert et al., 2008), locomotion (Kimmel et al., 2000), learning and memory (Upadhya et al., 2011b), anxiety and depression (Dandekar et al., 2009), sleep and nociception (Upadhya et al., 2011a).

CART neural circuitry in energy homeostasis

The best characterized role of CART is its involvement in energy homeostasis. Intracerebroventricular administration of CART peptide in rodents reduced food intake in fed as well as starved animals in a dose dependant manner (Kristensen et al., 1998). Chronic administration of CART inhibited food intake (Vrang et al., 2000). CART is abundantly expressed in hypothalamus of mammals, specifically in areas such as arcuate, lateral hypothalamic, paraventricular nuclei which are critical for energy homeostasis and regulation of feeding behavior (Gautvik et al., 1996; Koylu et al., 1998). CART is colocalized with alpha-melanocyte stimulating hormone (alpha-MSH), a food intake inhibitor in the arcuate nucleus (Vrang et al., 2002). CART expression decreased with starvation and increased with re-feeding/glucose administration (Mukherjee et al., 2012; Subhedar et al., 2011; Volkoff et al., 2005). Particularly in teleosts, central administration of CART reduced food intake in goldfish (Volkoff and Peter, 2000). Starvation reduced CART mRNA expression in goldfish, common carp,catfish and Atlantic salmon (Abbott and Volkoff, 2011; Subhedar et al., 2011; Volkoff et al., 2005; Volkoff and Peter, 2000). Hyperglycemic treatment increased CART mRNA levels in hypothalamus of rainbow trout (Conde-Sieira et al., 2010) and central administration of glucose increased CART immunoreactivity in ventral telencephalon of catfish (Subhedar et al., 2011).

CART knockout mice showed higher food intake compared to wild type mice. CART mRNA expression in arcuate nucleus was reduced after fasting (Kristensen et al., 1998) which recovered after refeeding (Germano et al., 2007). In leptin deficient ob/ob mice, CART levels were reduced however it increased with leptin treatment in starved rats, indicating that CART might mediate leptin borne adiposity related signals (Kristensen et al., 1998).

Though several studies suggest CART elicits anorexia, orexigenic effects of the peptide have also been reported. Injection of CART (55-102) into ventromedial arcuate nucleus of fasted rat elicited a delayed, but significant increase in feeding (Abbott et al., 2001). Over expression of CART or repeated intra arcuate nucleus injection of CART resulted in increase in food intake and body weight (Smith et al., 2008). These results suggest that CART has multiple roles in energy homeostasis depending on the circuitry. Such disparate roles cannot be distinguished by classical tools of lesions, electrical stimulation and pharmacological treatments as they are too

non-specific and affect the whole brain or large parts of brain, thus limiting comprehensive analysis of neural circuits.

Mechanism of CART action

Even though, CART was first discovered in 1995 by Douglass et al., the receptor for CART is still not known. Attempts to find the CART receptor were unsuccessful because of low affinity interactions owing to non specific binding in brain homogenates and slices. The evidence for existence of a CART receptor is shown by many active studies investigating the mechanism of CART action. CART binding initiates multiple signaling mechanisms. CART receptor is thought to be a GPCR coupled with $G_{i/o}$ because addition of pertussis toxin inhibits CART induced activation of ERK signaling pathway in AtT20 cells and CART induced inhibition of voltage dependant Ca^{2+} signaling in primary cell culture. The CART induced ERK signaling is inhibited by U0126, an inhibitor of MEK kinases. Further, in some hypothalamic neurons, central administration of CART induces phosphorylation of cyclic AMP response element binding protein (CREB).

The mechanism through which CART induces anorexia is still not clear. NMDA receptor activation activates ERK signaling (English and Sweatt, 1996). Administration of noncompetitive NMDA inhibitor MK801 reduced CART induced activation of ERK in dorsal telencephalon in zebrafish suggesting NMDA receptor might contribute to ERK activation by CART (Fig.1, Wakhloo et al., unpublished work). This indicates that simultaneous activation of NMDAR and CART pathway might synergistically activate a downstream signaling which phosphorylates ERK which further might induce anorexia.

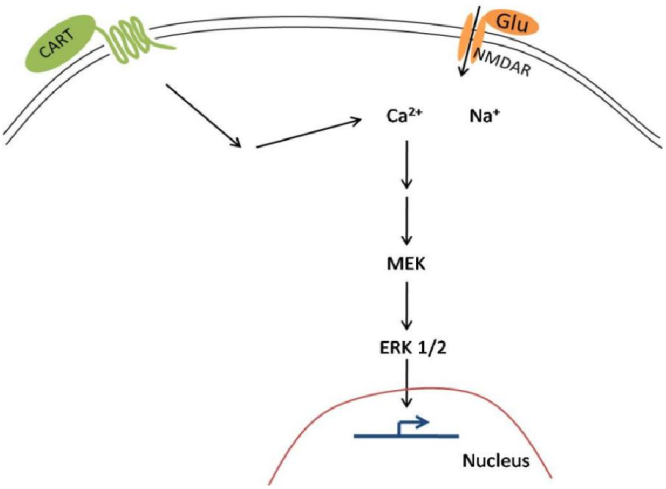

Figure 1: Mechanism of CART action in the Dm region of zebrafish. Binding of CART peptide and NMDAR activation together activates ERK pathway. (Wakhloo et al., unpublished work)

Sensory sensitivity in energy homeostasis

One prevailing hypothesis is that sensory sensitivity towards food cues such as gustation and olfaction is modulated because of changes in energy status and this change in sensitivity is reflected in behavioral response. Though this general hypothesis has been tested, the neural mechanism underlying this modulation is poorly understood. In hungry Drosophila, magnitude of olfactory signaling was enhanced resulting in a changed odor map which induces more robust food – search behavior (Root et al., 2011). Gustatory responses to sugar were enhanced in hungry flies because of dopamine neuromodulation (Inagaki et al., 2012). (Mousley et al., 2006) reported change in expression or activity of Neuropeptide Y (NPY) receptors in the olfactory epithelium with hunger level in axolotl and suggested that terminal nerve NPY might be involved in this modulation. NPY increased olfactory sensitivity in olfactory mucosa in fasted but not in fed rats (Negroni et al., 2012). Also NPY receptors were over expressed in olfactory mucosa of fasted rats as detected from western blot analysis (Negroni et al., 2012). These studies suggest a strong relation between nutritional processes and sensory sensitivity. With these data in background, we hypothesize that, NPY a strong orexigenic agent (Volkoff et al., 2005) might be involved in modulating olfactory sensitivity in zebrafish depending on the energy status. To test this, we built electro-olfactogram setup to record ensemble electrical activity of olfactory neurons and measure the magnitude of change in sensitivity.

Chapter 2

Materials and Methods

Animal handling and sampling procedures

All procedures were performed according to the guidelines of the Institutional Animal Ethics Committee (IAEC) of IISER, Pune, under the Committee for the Purpose of Control and Supervision of Experiments for Animals (CPCSEA), New Delhi, India. Wild-type Indian strain zebrafish (*Danio rerio*) were used in the present study. The fish were housed in multiplexed re-circulating tanks (Aquatic Habitats, USA) and maintained at 28.5°C under controlled light-dark conditions (14L/10D). Regular water quality checks were undertaken to maintain optimum water quality (hardness 100 - 300 mg/L of $CaCO_3$; alkalinity 50 - 300 mg/L of $CaCO_3$; nitrate < 20 mg/ml; pH 6-8; conductivity 180 – 350 µS).

Zebrafish breeding

Male and female zebrafish were identified and were kept physically separated in a breeding tank. Next day, during the onset of light, the separator was removed and they were allowed to mate. The fertilized eggs were then collected and kept in E3 medium (5 mM NaCl, 0.17 mM KCl, 0.33 mM $CaCl_2$, 0.33 mM $MgSO_4$, 0.00001% [w/v] methylene blue) at 28.5°C till 7 dpf.

Preparation of cDNA

RNA was extracted from zebrafish brains which were used to prepare cDNA. Zebrafish were deeply anesthetized with 2-phenoxy ethanol (1:2000), the brains dissected out and immediately frozen in liquid nitrogen. 1 ml of TRIzol® Reagent (Invitrogen, Carlsbad, CA, USA) was added to the frozen tissue and homogenized. After 5 min incubation at room temperature, 0.5 ml of chloroform was added and mixed thoroughly. The tubes were centrifuged for 15 min at 12000 g, 4°C and the upper aqueous layer was transferred to a fresh RNase free centrifuge tube. The RNA was precipitated by adding 0.5 ml of isopropanol for 1 hr at -20°C. Following centrifugation for 10 min at 12000 g, 4°C and a 70% ethanol wash, the RNA was

suspended in nuclease free water. DNase 1 (Promega, Madison, WI, USA) was added for 15 min to digest the residual DNA. The first strand cDNA was synthesized from RNA by RT-PCR using oligo-dT as primers and Moloney murine leukemia virus reverse transcriptase (Invitrogen, Carlsbad, CA). This cDNA was further used as a template for amplifying different genes.

Probe preparation

Different CART genes were amplified from the cDNA using specific primers, which included T3 and T7 RNA polymerase promoter sequences for *in vitro* transcription. Sense and antisense probes were synthesized using T7 and T3 RNA polymerase (Promega, Madison, WI, USA), respectively, in the presence of dNTPs containing digoxigenin (DIG) labeled UTPs (Roche Applied Sciences, Indianapolis, IN). The probes were treated with DNase 1 (Promega, Madison, WI, USA) for 15 min to remove the DNA template and were ethanol precipitated overnight using lithium chloride. The probes were resuspended in nuclease free water after a 70% ethanol wash. Sense probes were used to establish the specificity of the antisense probes. Specific probe information can be found in Table 1.

Gene	Accession ID no.	Probe position (bp)
CART 1	XM_686251.3	3- 317
CART 2	NM_001017570.1	87- 399
CART 3	DN857240.1	49 - 189
CART 4	NM_001082932.1	16 - 565

Table 1. Probe Information
Accession ID for the Genbank database as well as the corresponding base pairs the probe binds to on the mRNA sequence are provided.

In situ hybridization

The *in situ* hybridization (ISH) protocol has been described previously (Kuhn and Koster, 2010). Adult zebrafish were deeply anesthetized with 2-phenoxy ethanol

(1:2000) and the brains were dissected out. The brains were fixed in 4% paraformaldehyde overnight. Following five washes (5 min each) with PTW buffer (0.1% Tween 20 in PBS) the brains were digested with proteinase K (10 µg/ml) for 40 min (without shaking), washed twice briefly with glycine (2 mg/ml) solution and fixed again in 4% paraformaldehyde for 20 min. The brains were washed five times (5 min each) in PTW buffer and pre-hybridized for 1 hr at 60°C with the hybridization buffer (50% formamide, 50 µg/ml heparin, 5X SSC, 5 mg/ml yeast total RNA and 0.1% Tween 20). 10 µl of DIG labeled probes in 200 µl hybridization buffer were incubated at 90°C for 10 min (to disrupt RNA secondary structures) and were added to the tissue for overnight hybridization at 60°C. Following hybridization, the probes were removed and the brains were washed twice with 50% formaldehyde/2X SSC/0.1% Tween 20, once with 2X SSC/0.1% Tween 20 and subsequently twice with 0.2X SSC/0.1% Tween 20 at 60°C. The brains were then embedded in 3% agarose blocks and sectioned (100 µm) using a vibratome (VT 1200; Leica, Germany). The sections were transferred to slides, dried, blocked with 10% normal goat serum for 1 hr (at room temperature) and then incubated overnight at 4°C with sheep anti-DIG alkaline phosphatase conjugated antibody (1:2000) (Roche Applied Sciences, Indianapolis, IN) diluted in 10% normal goat serum. Next, the sections were washed five times with PTW buffer and twice with coloration buffer (100 mM Tris-HCl pH 9.5, 50 mM $MgCl_2$, 100 mM NaCl, 0.1% Tween 20). DIG labeled probes were detected using a chromogen mixture containing NBT/BCIP in the coloration buffer. The reaction was continuously monitored and on achieving the desired intensity, the reaction was stopped by washing thrice with PTW buffer. The sections were mounted in glycerol medium (0.5% N-propyl gallate, 20 mM Tris pH 8, 70% glycerol and 1 µg/ml 4',6-diamidino-2-phenylindole (DAPI)) and were either processed for imaging or stored at 4°C. Bright field/epifluorescence observations and photomicrography were undertaken with an upright fluorescence microscope (Axioimager Z1, Carl Zeiss, Germany). The images were adjusted for size, brightness and contrast using Photoshop (Adobe Systems, San Jose, CA, USA). Neuroanatomical areas in adult zebrafish brain were identified based on earlier descriptions (Berman et al., 2009; Mukherjee et al., 2012; Wullimann et al., 1996; Yokobori et al., 2012), DAPI and/or cresyl violet staining.

Starvation experiments

The fed control group consisted of fish that were anesthetized and killed two hours after feeding. The other group consisted of adult zebrafish starved for 5 days. The brains of both the groups were dissected out in parallel and were processed for *in situ* hybridization. All the processing steps, including color development of the starved and control brains were undertaken in identical conditions using the same solutions. Minimum of five fishes per group were employed for quantification of cells.

Image analysis

The change in expression pattern of all four CART genes (CART 1, CART 2, CART 3 and CART 4) upon starvation was determined using ISH. The CART positive cells at different regions were manually counted in both control and starved group. At least three independent experimental replicates were evaluated in each group. The person scoring the slides was blind to the treatment and two independent scorers counted the neurons. To avoid over estimation of cell count due to sectioning, the cell numbers were corrected using Abercrombie's method (Abercrombie, 1946) by using the equation $N = (nxT)/(T+d)$ where N is the corrected cell number, T is the thickness of section, n is the actual cell count and d is the mean diameter of the cells. The data were statistically analyzed using two tailed, unpaired Student's t-test. Graphs were plotted using the Graphpad Prism 5.0 statistical software.

Cresyl violet and DAPI staining

The sections were air dried for 15 min before the addition of 0.2% cresyl violet solution (in distilled water; Sigma-Aldrich) for 1-4 min. The slides were differentiated in distilled water for 3-5 min, washed with 70% ethanol for 1 min, with 90% ethanol for 1 min, and twice with 100% ethanol for 1 min. The sections were cleared in xylene for 3-5 min and mounted in DPX. For DAPI staining, the sections were placed in mounting media (0.5% N-propyl gallate, 20mM Tris pH 8, 70% glycerol) containing 4',6-diamidino-2-phenylindole (DAPI, 1µg/ml; Sigma-Aldrich). The specimens were imaged with an upright fluorescence microscope (Axioimager Z1, Carl Zeiss, Germany) with appropriate excitation and emission filters.

Sequence alignment

Basic local alignment search tool (BLAST) analysis of the National Centre for Biotechnology Information (NCBI) was used to test the specificity of the probes against the zebrafish genome (http://blast.ncbi.nlm.nih.gov/Blast.cgi). The scoring parameter included 1/-2 match/mismatch with linear gap cost. Clustal Omega, multiple sequence alignment tool by European Bioinformatics Institute of European Molecular Biology Laboratory was used to align and determine the similarity between zebrafish and mammalian CART peptide sequences.

(http://www.ebi.ac.uk/Tools/services/web/toolform.ebi?tool=clustalo)

Chapter 3

Differential Distribution and Energy Status Dependant Regulation of the Four CART Genes*

Zebrafish is an attractive model system to study neural circuits because of its ease in genetic manipulations. Also zebrafish are small and transparent making the brain optically accessible to monitor and perturb neuronal activity (Portugues et al., 2013). Genomic duplication events in teleost evolution may have given rise to multiple CART genes as revealed by recent genomic studies. Two different CART genes are present in goldfish and PCR based strategies revealed non uniform abundance of transcripts in different brain regions and their differential regulation following starvation (Volkoff and Peter, 2001). Six CART genes have been identified in medaka and their distribution and response to starvation were assessed using qPCR (Murashita and Kurokawa, 2011). But, both these studies lack spatial resolution as they isolate mRNA from relatively large brain tissue volumes. While four CART genes are found in zebrafish Nishio et al., (2012) reported down regulation of CART 4 expression in a cannabinoid receptor 1 dependent manner in fasted zebrafish larvae. Mukherjee et al., (2012), documented the ontogeny of CART peptidergic system in zebrafish and demonstrated that glucose responsive CART circuits appear early in development. Expansion of CART family may confer differential functions, specific or redundant to the CART gene products. In an attempt to study specific CART neural circuits involved in energy homeostasis, we map the expression of the four CART genes in adult zebrafish brain. We also identify neurons which respond to starvation which could be used as a starting point in a gene and circuit specific investigation of CART's role in energy homeostasis.

*

- This chapter forms a part of the following publication

Akash, G., Kaniganti, T., Tiwari, N.K., Subhedar, N.K., and Ghose, A. (2013). Differential distribution and energy status-dependent regulation of the four CART neuropeptide genes in the zebrafish brain. J Comp Neurol.

Results

Alignment of zebrafish CART amino acid sequences

Alignment of the four zebrafish CART peptides with the 55 – 102 fragment of rat CART peptide fragment (Fig. 2) identified the zebrafish CART 2 to have the most similarity with mammalian CART (79.17% identity). CART 3 and CART 1 share 72.92% and 70.83% identity with mammalian CART, respectively. CART 4 is the most divergent with only 55.32% identity with rat CART.

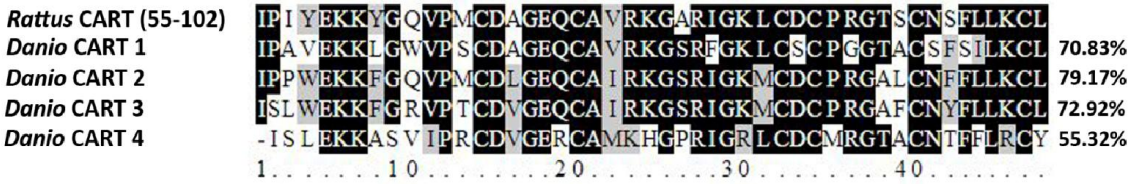

Figure 2: Alignment of zebrafish CART amino acid sequences

CLUSTAL Omega alignment of peptide sequences of zebrafish CART 1 (ADB12484.1), CART 2 (ADB12485.1), CART 3 (ADB12486.1), CART 4 (ADB12487.1) and rat CART 55-102 (AAA87897.1). Black background represents identical residues, grey background represents similar residues and white background represents different residues. The percentage identity with rat CART (55-102) is indicated on the right.

Specificity of probes

Probes specific to each of the four CART mRNA were used to determine the expression of different CART genes. Specificity of probes for all genes was checked using sense and antisense probe *in situ* hybridization. Lack of signals in the brain regions using sense probe, where a strong signal is seen using antisense probe showed the specificity of antisense probe binding.

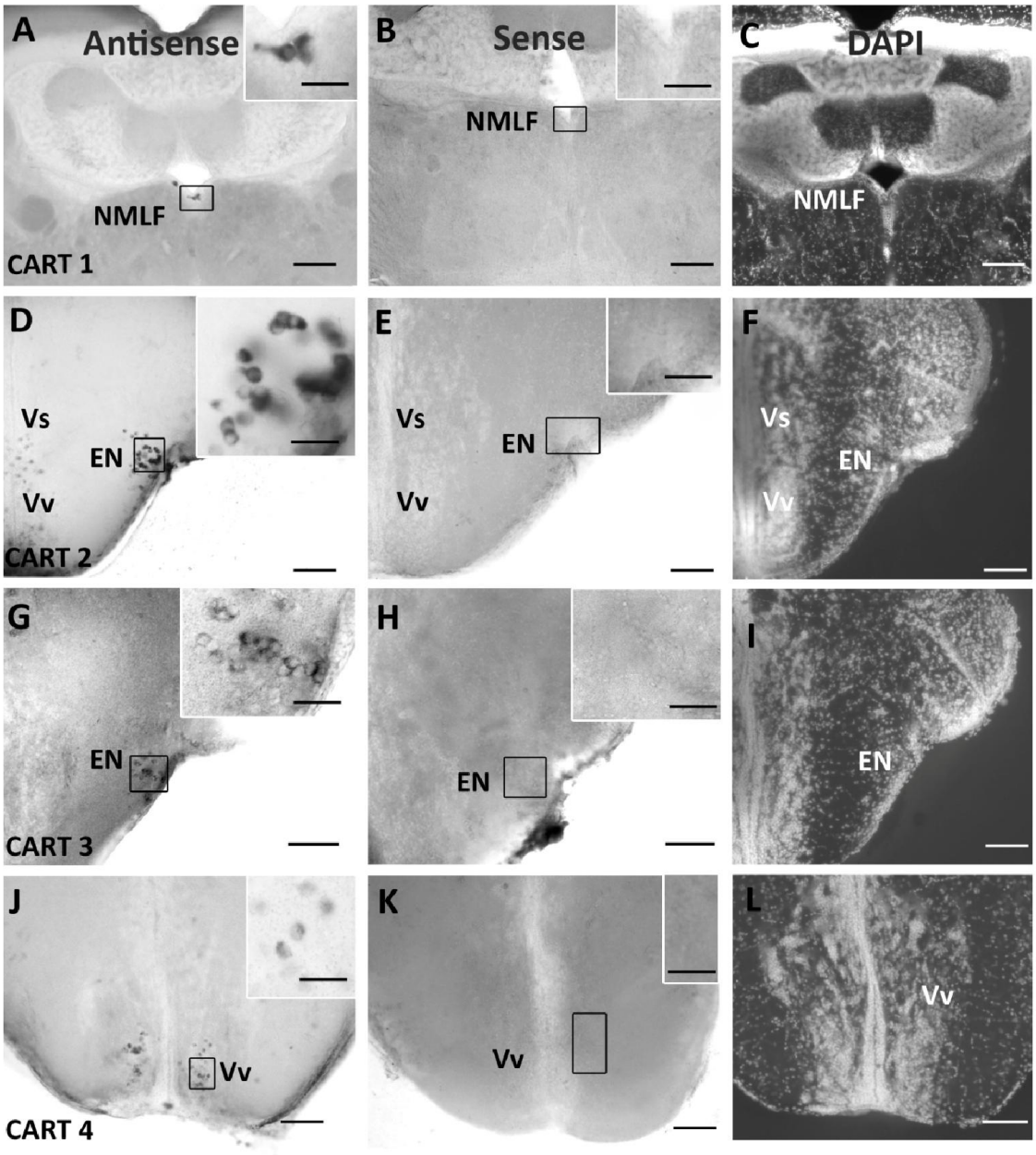

Figure 3: Specificity of probe binding

Brain sections were treated with antisense (**A, D, G, J**) and sense probes (**B, E, H, K**) to control for the non-specific labeling. DAPI staining indicates the distribution of nuclei demarcating the different regions in the brain sections (**C, F, I, L**). **A:** CART 1antisense probe labels the nucleus of the medial longitudinal fascicle (NMLF). **D:** CART 2 antisense probe labeling is seen in the entopeduncular nucleus (EN), ventral nucleus of the ventral telencephalic area (Vv) and the supracommissural nucleus of the ventral telencephalic area (Vs). **G:** CART 3 mRNA containing cells in the EN. **J:** CART 4 labeling is seen in the Vv area. No labeling was seen in the CART 1 (**B**), CART 2 (**E**), CART 3 (**H**) and CART 4 (**K**) sense probe treated sections. Insets are higher magnification micrographs of the boxed regions. Scale bar = 100 µm (**A-L**); 25 µm in the insets.

Distribution of CART mRNA in the zebrafish

The distribution of different CART mRNAs is schematically represented in Figs. 4, 5, 7, 8 and 11. The identity of the various brain areas having CART mRNA expressing neurons was determined from earlier studies and comparisons with cresyl violet and/or DAPI staining (Castro et al., 2009; Mueller and Wullimann, 2005; Mukherjee et al., 2012; Wullimann et al., 1996; Yokobori et al., 2012).

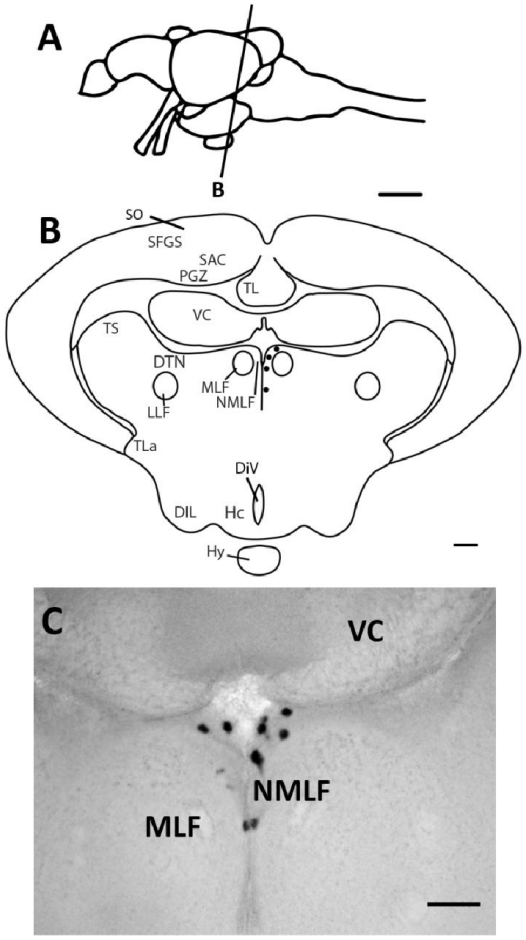

Figure 4: CART 1 mRNA expression

CART 1 mRNA expression pattern in adult zebrafish brain. **A:** lateral view of the brain indicating the section level (**B**) represented in the corresponding transverse section showing CART 1 mRNA containing cells (black dots). **C:** Transverse section showing CART 1 mRNA containing cells in the NMLF. For abbreviations, see list. Scale bar **A**= 1000 µm; **B** = 50 µm; **C** = 100 µm.

Expression of CART mRNAs in the forebrain

Granule cells of the olfactory bulb showed CART 2 and CART 4 mRNA expression (Figs. 5B, 6A, 8B). CART 2 mRNA was expressed in the dorsolateral region of the rostral fourth of the telencephalon (Figs. 5B,C, 6B). CART 4 mRNA expressing neurons were confined to the Dl region of the telencephalon, extending caudally from the level of the anterior commissure (AC; Figs. 8E,F, 9C). The ventral telencephalon has several regions that express CART mRNA. The Vs and Vv of the ventromedial telencephalon showed CART 2 expression. CART 4 mRNA containing cells were found extensively in the Vv, and sparsely in Vd region (Figs. 5D,E, 6C,C',D, 8C,D, 9A). Across the entire brain, CART mRNA expression was most abundant in the entopeduncular nucleus (EN) of the ventrolateral

telencephalon. A specific pattern of CART mRNA distribution was found along the rostro-caudal axis of the EN. While CART 3 mRNA was detected throughout the EN (Figs. 7B-E), CART 2 expression was more rostral, but limited to the level of the AC (Figs. 5D,E, 6C,D). CART 4 expression was confined to a sparse population in the caudal regions of the EN, from the AC level extending to the level of the optic chiasma (Figs.8E,F, 9B).

Preoptic area (POA) consisted of cells expressing CART 2 and CART 4. Few CART 2 mRNA expressing cells were seen in the ventral part of the PPa (anterior part of parvocellular preoptic nucleus; Figs. 5E, 6D) and in the caudal PPp (posterior part of the parvocellular preoptic nucleus; Figs. 5F, 6E). CART 4 mRNA containing cells were detected in the PPp and in dorsal region of PPa (Figs. 8E,F, 9B).

Within the thalamic regions, CART 2 expressing cells were detected in the ventromedial thalamic nucleus (VM; Figs. 5G-I, 6F-H) and a few cells were located immediately above the horizontal commissure (HC; Figs. 5H, 6G) in the same coronal section plane. A cluster of CART 2 mRNA-positive neurons was seen in the central posterior thalamic nucleus (CP), preglomerular nucleus (PG), the anterior thalamic nucleus (A), ventral accessory optic nucleus (VAO) (Figs. 5I-K, 6H,K,P). CART 2 and CART 4 containing isolated perikarya were detected in the periventricular nucleus of the posterior tuberculum (TPp; Figs. 5J, 6K, 8I, 9E).

Amongst the hypothalamic nuclei, rostrally at the level of the optic chiasma (OC), CART 2 and CART 4 mRNAs were detected in the region of the suprachiasmatic nucleus (SCN; Figs. 5G, 6F, 8G, 9D). In the tuberal region, CART 2 and CART 4 mRNA containing cells, with distinctly outlined cell nuclei, were seen in the nucleus lateralis tuberis (NLT; Figs. 5I,J, 6O,O', 8I,J, 9F). CART 2 mRNA was seen in the posterior tuberal nucleus (PTN) neurons located close to the mid-line, just above the diencephalic ventricle (DiV) (Figs. 5K, 6L,L''). CART 4 mRNA containing cells were seen in the nucleus recessus lateralis (NRL) as a group of small neurons spread in the vicinity of the lateral hypothalamic recesses of the third ventricle (Figs. 8K, 9G). However, CART 2 mRNA was confined to a discrete cluster of NRL neurons located at the lateral edge of the lateral recesses (Figs. 5K, 6L,L'). Few labeled cells expressing CART 2 and 4 mRNAs were also observed in the caudal zone of the periventricular hypothalamus (Hc; Figs. 5K,L, 6L,L''', 8L, 9I).

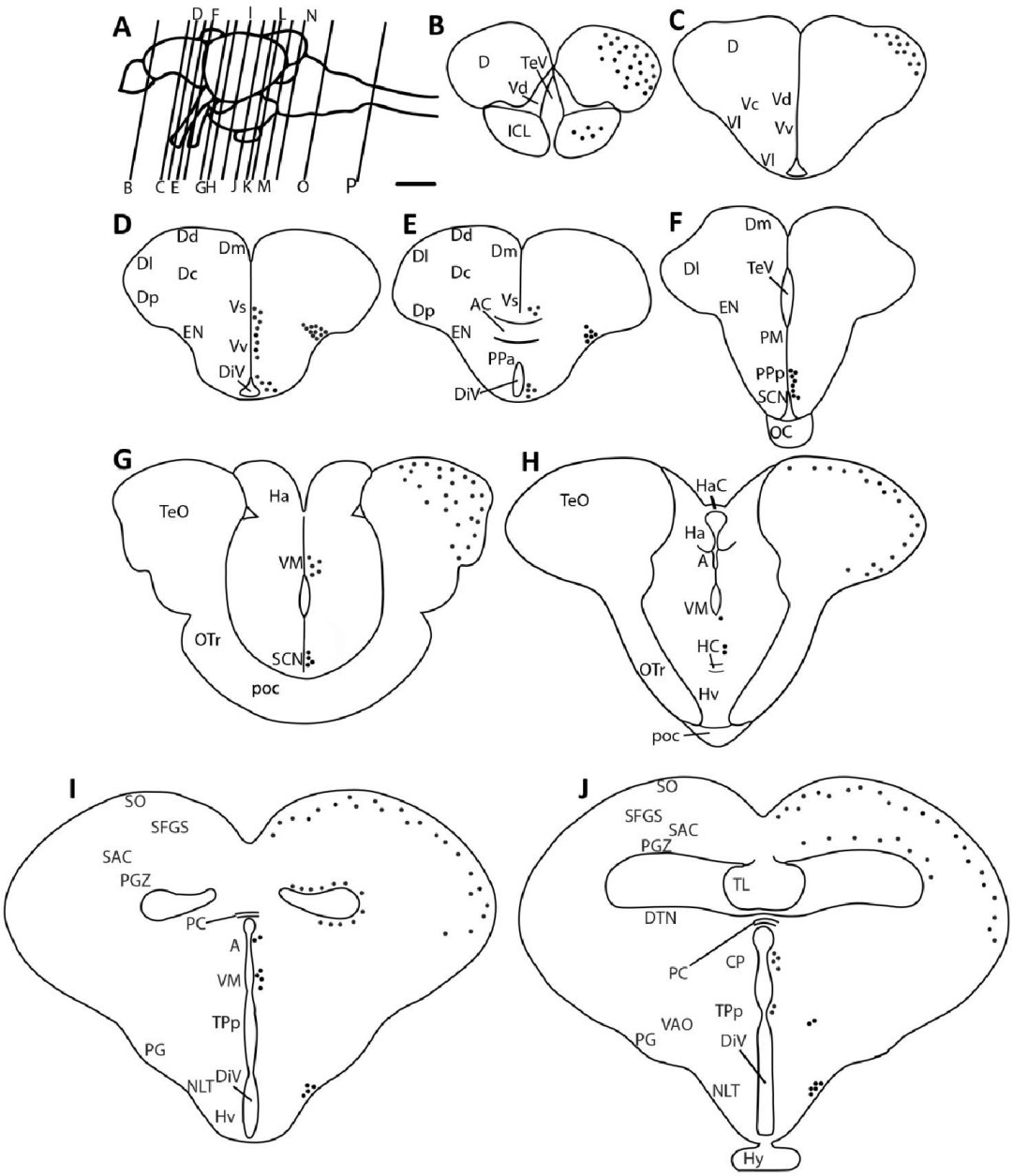

Figure 5: Schematic of CART 2 mRNA expression

Schematic drawings of CART 2 mRNA containing cells in the CNS of the adult zebrafish. **A:** lateral view of the brain indicating the levels of corresponding transverse sections (**B-P**) showing CART 2 mRNA containing cells (black dots). For abbreviations, see list. Scale bar **A** = 1000 µm; 50 µm in **N** (applies to **B-P**).

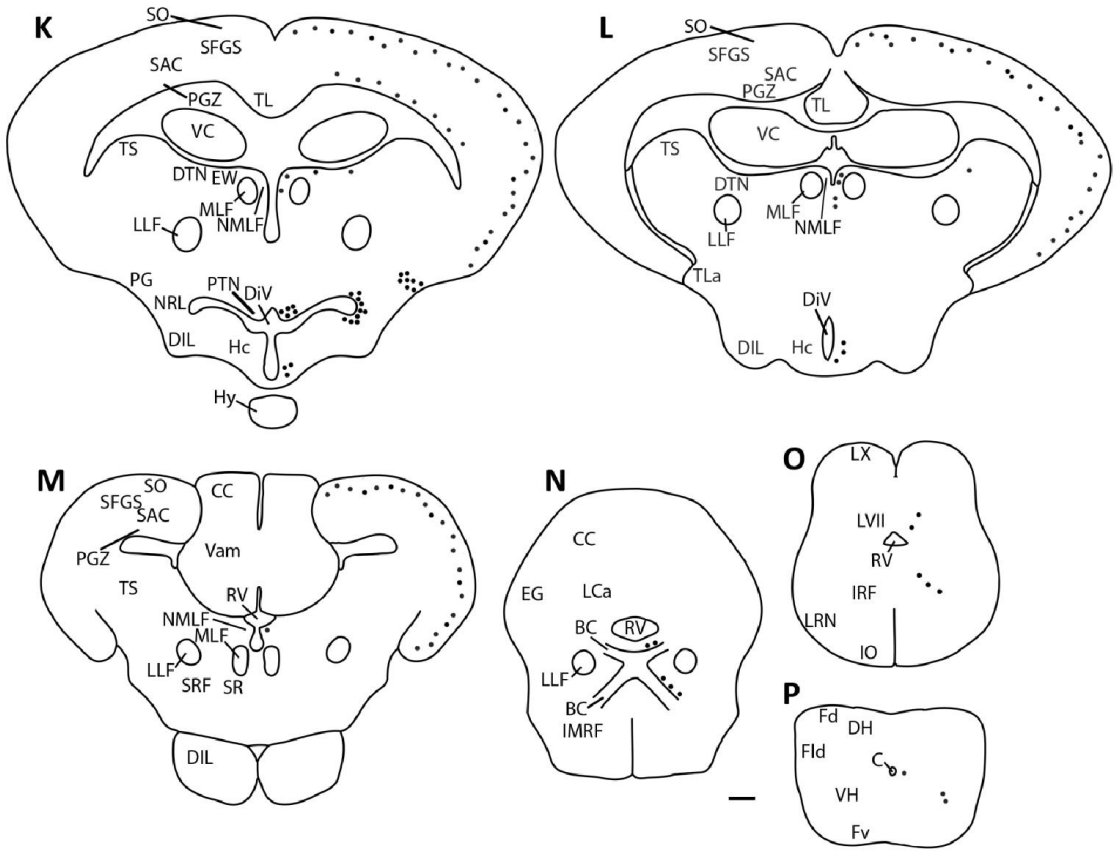

Figure 5 continued

Expression of CART mRNAs in the midbrain

Only CART 2 mRNA was expressed in the optic tectum and it showed laminar arrangement in the stratum opticum (SO), and the stratum fibrosum et griseum superficiale (SFGS; Figs. 5H-M, 6M). Further, CART 2 positive neurons were seen in the periventricular gray zone of the optic tectum (PGZ), in the vicinity of the ventricular lumen (Figs. 5I,J, 6N). Dorsal tegmental nucleus (DTN) of synencephalon and the torus semicircularis (TS) consisted of a small number of CART 2 and CART 4 mRNA expressing cells (Figs. 5K,L, 8K, 9H). Also isolated CART 2 containing neurons were also detected in the Edinger-Westphal nucleus (EW; Figs. 5K, 6J). In the dorsal pretegmental area, close to the mid-line, CART 1, CART 2 and CART 4 transcripts were seen in the nucleus of the medial longitudinal fascicle (NMLF; Figs. 4B,C,5K-M,6Q, 8M, 9J). CART 1 positive cells were seen only in this region in the whole adult zebrafish brain. CART 3 mRNA containing cells were not detected in the midbrain of the zebrafish.

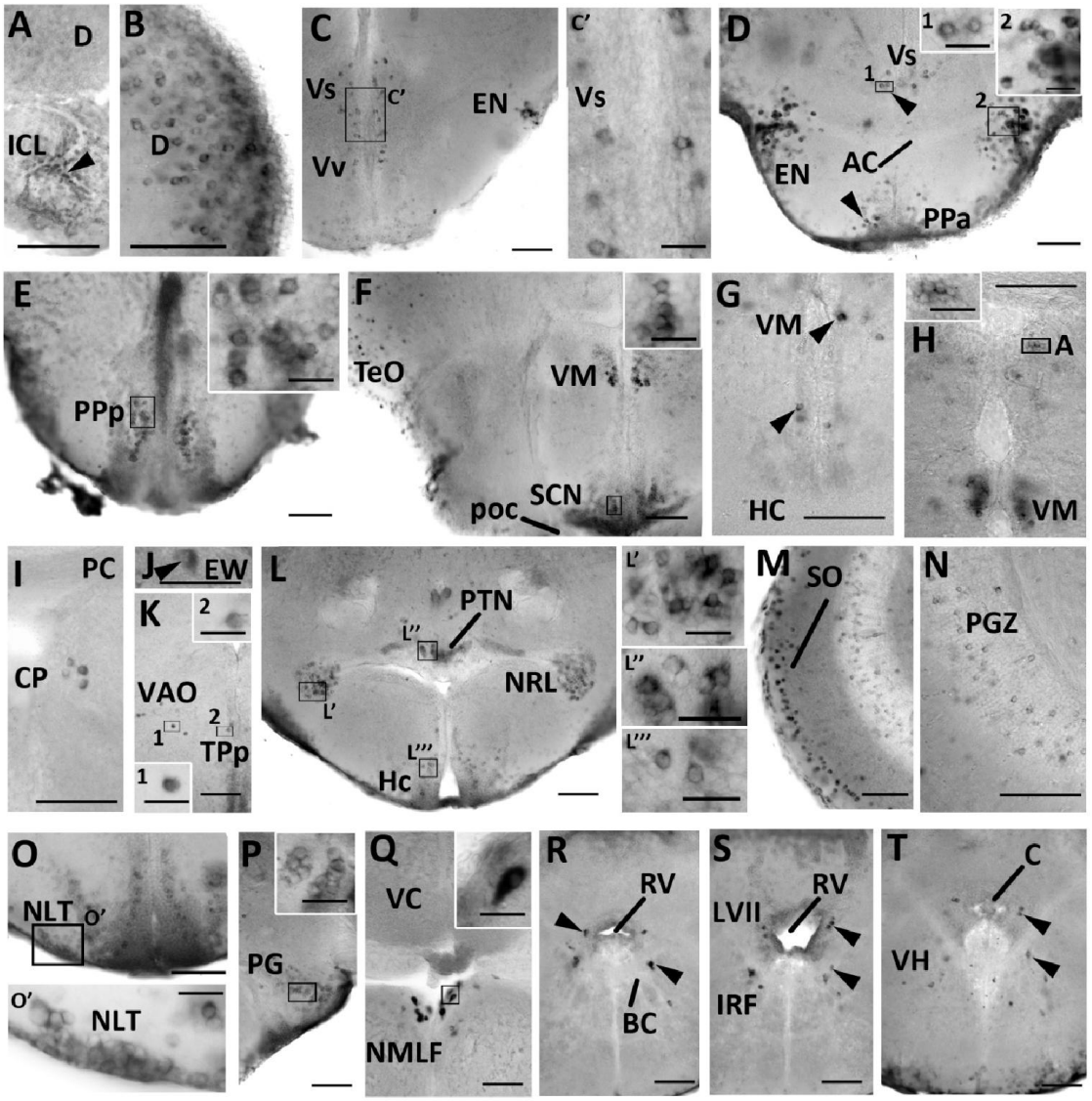

Figure 6: CART 2 mRNA expression

Rostrocaudal series of transverse sections (**A-T**) of the CNS of adult zebrafish showing CART 2 mRNA containing cells. **A:** CART 2 labeling is seen in the internal cell layer of olfactory bulb (ICL; arrowhead). **B:** Many cells are seen in the dorsal telencephalic area (D). **C,D:** Dense population of CART 2 containing cells is seen in the entopeduncular nucleus (EN) and dispersed cells are seen in the ventral telencephalic area (Vv**;** **C**) and the supracommissural nucleus of the ventral telencephalic area (Vs**;** arrowhead; **C,C',D**). CART 2 positive cells are seen in the anterior part of parvocellular preoptic nucleus (PPa; arrowhead; **D**), posterior part of the parvocellular preoptic nucleus (PPp; **E**), ventromedial thalamic nucleus (VM; arrowhead; **F,G,H**) and in the suprachiasmatic nucleus (SCN; **F**). Several cells are distributed in the optic tectum (TeO; **F**). Few cells are seen in the anterior thalamic nucleus (A; **H**), central posterior thalamic nucleus (CP; **I**), Edinger-Westphal nucleus (EW; arrowhead; **J**), ventral accessory optic nucleus (VAO; **K**) and the periventricular nucleus of posterior tuberculum

(TPp; **K**). **L:** Three different neuronal groups containing CART 2 mRNA are seen in the nucleus recessus lateralis (NRL; **L'**), caudal zone of periventricular hypothalamus (Hc; **L'''**) and the posterior tuberal nucleus (PTN; **L''**). *In situ* labeling was widely seen in the stratum opticum (SO; **M**), and in the periventricular gray zone of optic tectum (PGZ; **N**). Few CART 2 positive cells are seen in the nucleus lateralis tuberis (NLT; **O, O'**) and in the preglomerular nucleus (PG;**P**). Large, intense labeling is seen in nucleus of the medial longitudinal fascicle (NMLF; **Q**). Few cells containing CART 2 mRNA are present outlying the brachium conjunctivum (BC; arrowhead; **R**), the facial lobe (LVII; arrowhead; **S**) andthe inferior reticular formation (IRF; arrowhead; **S**). In the spinal cord, labeled cells are seen near the central canal (C; arrowhead; **T**) and in the ventral horn (VH; arrowhead; **T**). Insets are higher magnification micrographs of the boxed regions. Scale bar = 100 µm in **A-T**; 25 µm in the insets.

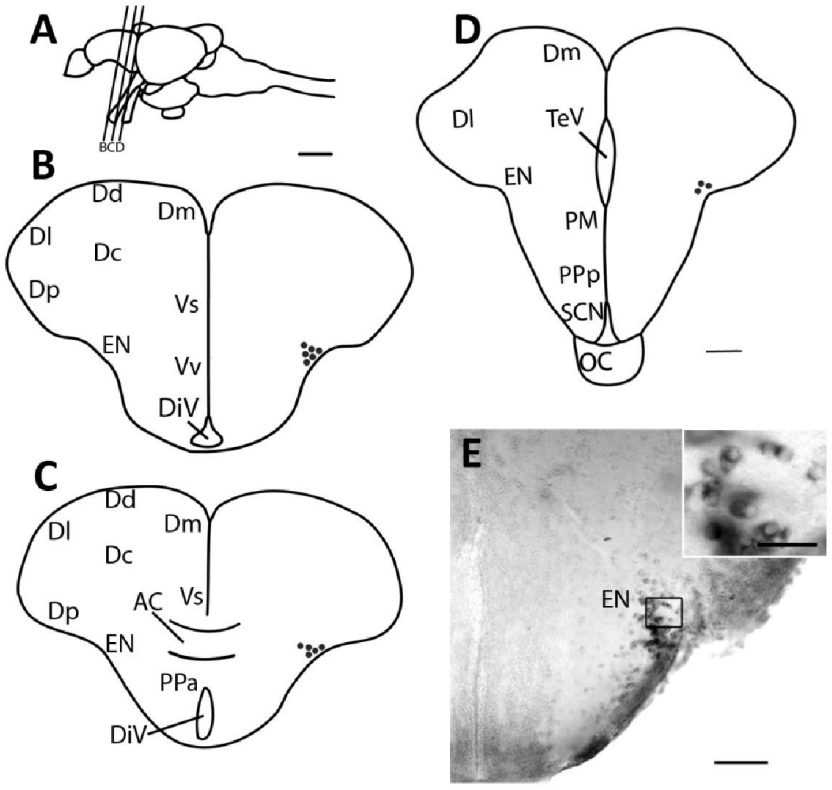

Figure 7: CART 3 mRNA expression

CART 3 mRNA expression pattern in adult zebrafish brain. **A:** lateral view of the brain indicating the level of the transverse sections (**B,C,D**) showing CART 3 mRNA containing cells (black dots). Transverse section (**E**) shows CART 3 mRNA containing cells in the entopeduncular nucleus (EN). For abbreviations, see list. Scale bar **A** = 1000 µm; **B-D** = 50 µm; **E** = 100 µm; 25 µm in the inset.

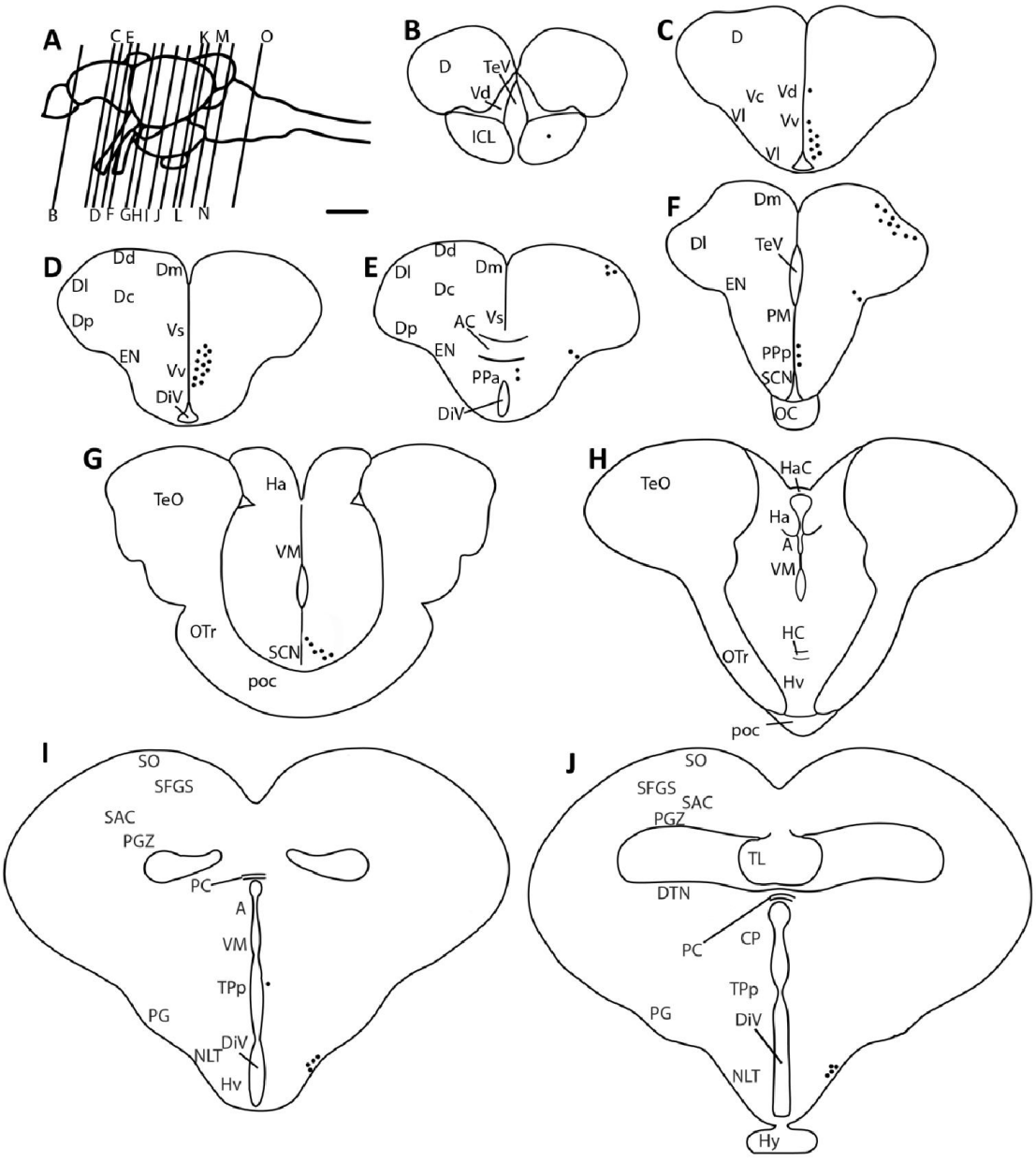

Figure 8: Schematic of CART 4 mRNA expression

Schematic drawings of CART 4 mRNA containing cells in the CNS of the adult zebrafish. **A:** lateral view of the brain indicating the levels of corresponding transverse sections (**B-O**) showing CART 4 mRNA containing cells (black dots). For abbreviations, see list. Scale bar**A** = 1000 µm; 50 µm in **N** (applies to **B-O**).

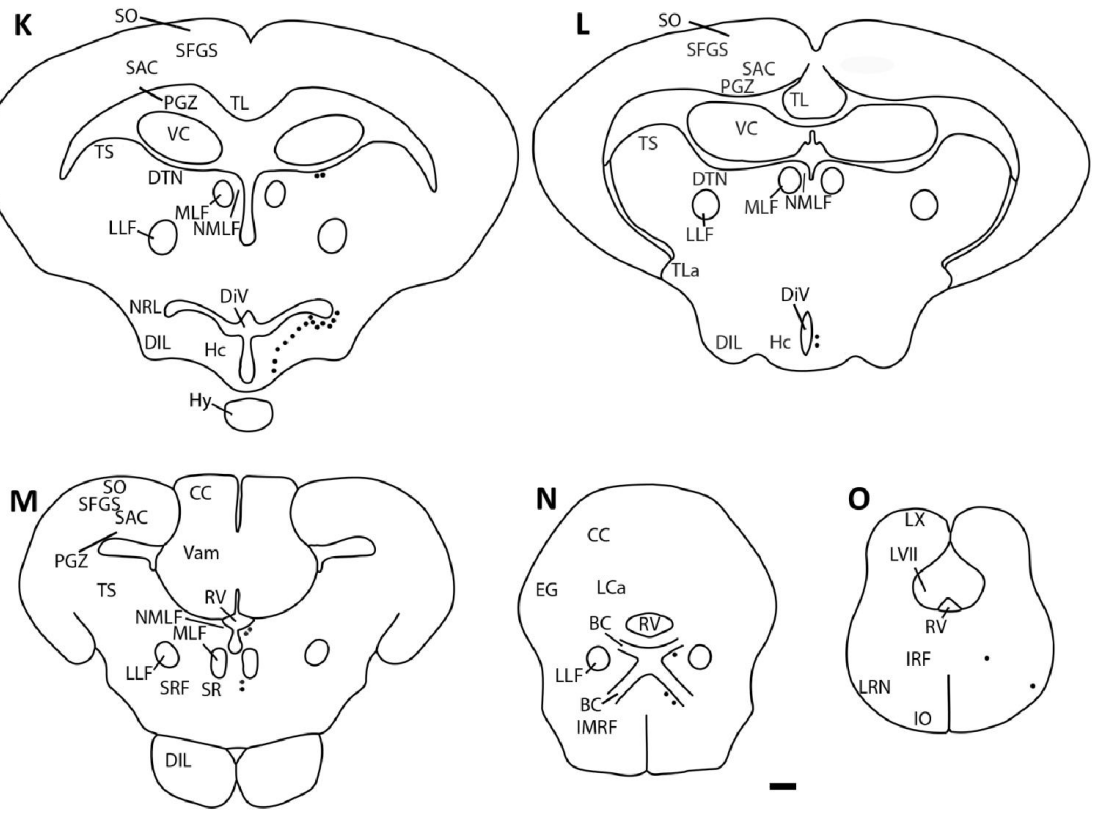

Figure 8 continued

Expression of CART mRNAs in the hindbrain and spinal cord

Only CART 2 and CART 4 mRNA containing cells were seen in the hindbrain. Some CART 2 mRNA expressing neurons were seen in the facial lobe (LVII; Figs. 5O, 6S) and sparsely distributed cells were seen in the inferior reticular formation (IRF) and the immediate vicinity of the brachium conjunctivum (BC) regions of the medulla oblongata (MO; Figs. 5N,O, 6R,S).

In addition, CART 4 mRNA was seen in the lateral reticular nucleus (LRN), IRF, in the vicinity of the BC and in the superior raphe (SR) regions of the medulla (Figs. 8M-O, 9J-L). CART 1 or 3 mRNA expression was not detected in the hindbrain.

In the spinal cord, few CART 2 containing cells were seen in the vicinity of the central canal (C) and in the ventral horn (VH) while no other CART containing cells were detected (Figs. 5P, 6T).

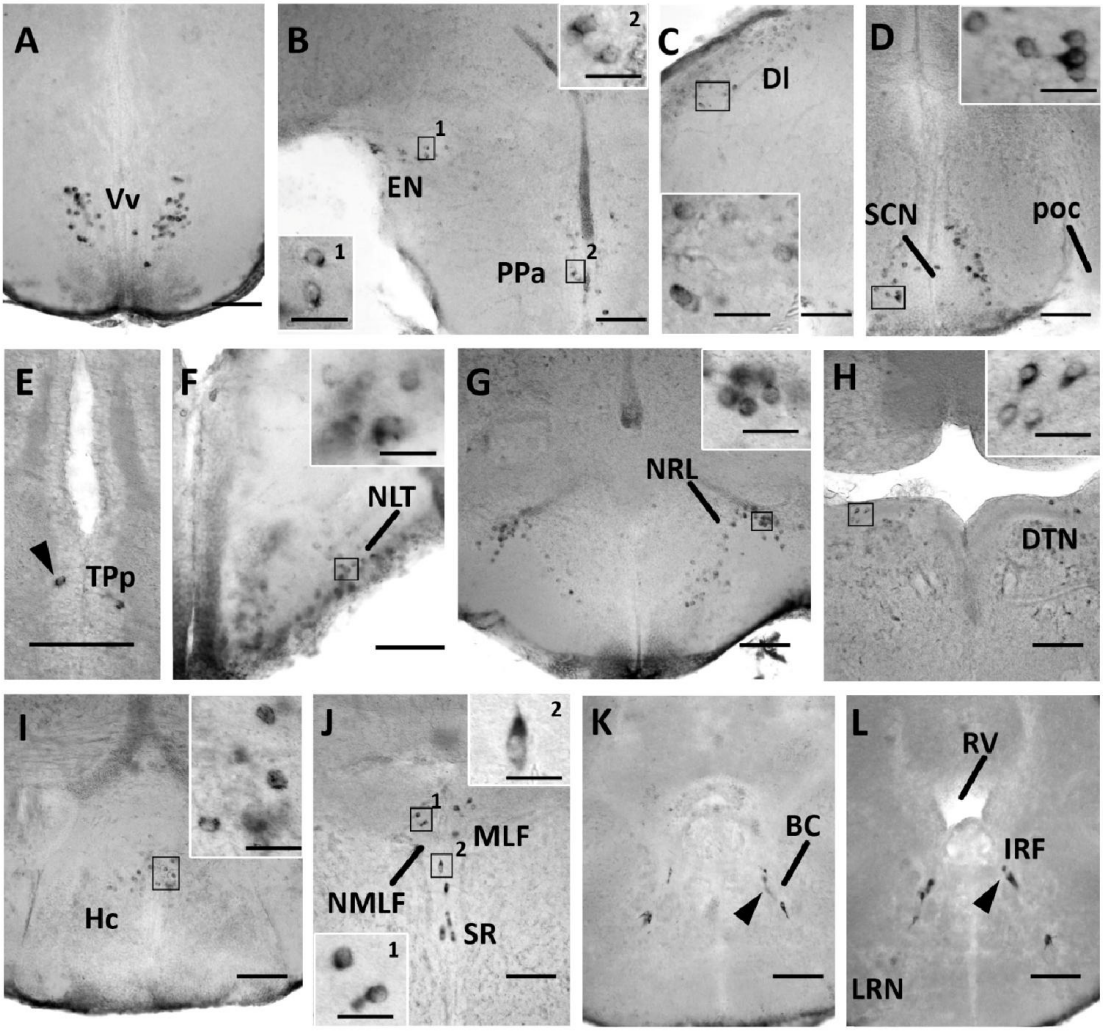

Figure 9: CART 4 mRNA expression

Rostrocaudal series of transverse sections **(A-L)** of the CNS of adult zebrafish showing CART 4 mRNA containing cells. CART 4 mRNA containing cells are seen in the ventral nucleus of the ventral telencephalic area (Vv; **A**), entopeduncular nucleus (EN; **B**), anterior part of parvocellular preoptic nucleus (PPa; **B**) and in the lateral zone of the dorsal telencephalic area (Dl; **C**). CART 4 labeling is seen in the suprachiasmatic nucleus (SCN; **D**) and the periventricular nucleus of posterior tuberculum (TPp; arrowhead; **E**). CART 4 positive cells are seen in the nucleus lateralis tuberis (NLT; **F**) and the nucleus recessus lateralis (NRL; **G**). Few CART 4 mRNA containing cells are observed in the dorsal tegmental nucleus (DTN; **H**) and the caudal zone of periventricular hypothalamus (Hc; **I**). CART 4 mRNA containing cells are seen in the nucleus of the medial longitudinal fascicle and superior raphe (NMLF, SR; **J**). Few CART 4 positive cells are seen near the brachium conjunctivum (BC; arrowhead; **K**) and in the inferior reticular formation (IRF; arrowhead; **L**). Scale bar = 100 µm in **A -L**; 25 µm in the insets.

Energy status dependant regulation of CART gene expression

Following starvation for a period of 5 days, the number of CART 2 mRNA expressing EN neurons was significantly reduced ($p < 0.005$) as compared to that in the control (Figs. 10D-F). In the tuberal hypothalamus, the CART 2 mRNA expressing group of neurons in the NRL, located laterally to the lateral recesses, showed complete loss of mRNA expression in the starved fish (Figs. 10G-I; $p < 0.005$). Other populations of CART 2, including those in the hypothalamic NLT, PTN and Hc areas did not change in number (Figs. 10G-I). The number of CART 4 containing neurons of the NLT was significantly reduced upon starvation ($p < 0.05$), but other CART 4 populations were not affected (Figs. 10M-Q). The number of CART 1 containing neurons in the NMLF and CART 3 mRNA neurons in the EN did not change with starvation (Figs. 10A-C,J-L).

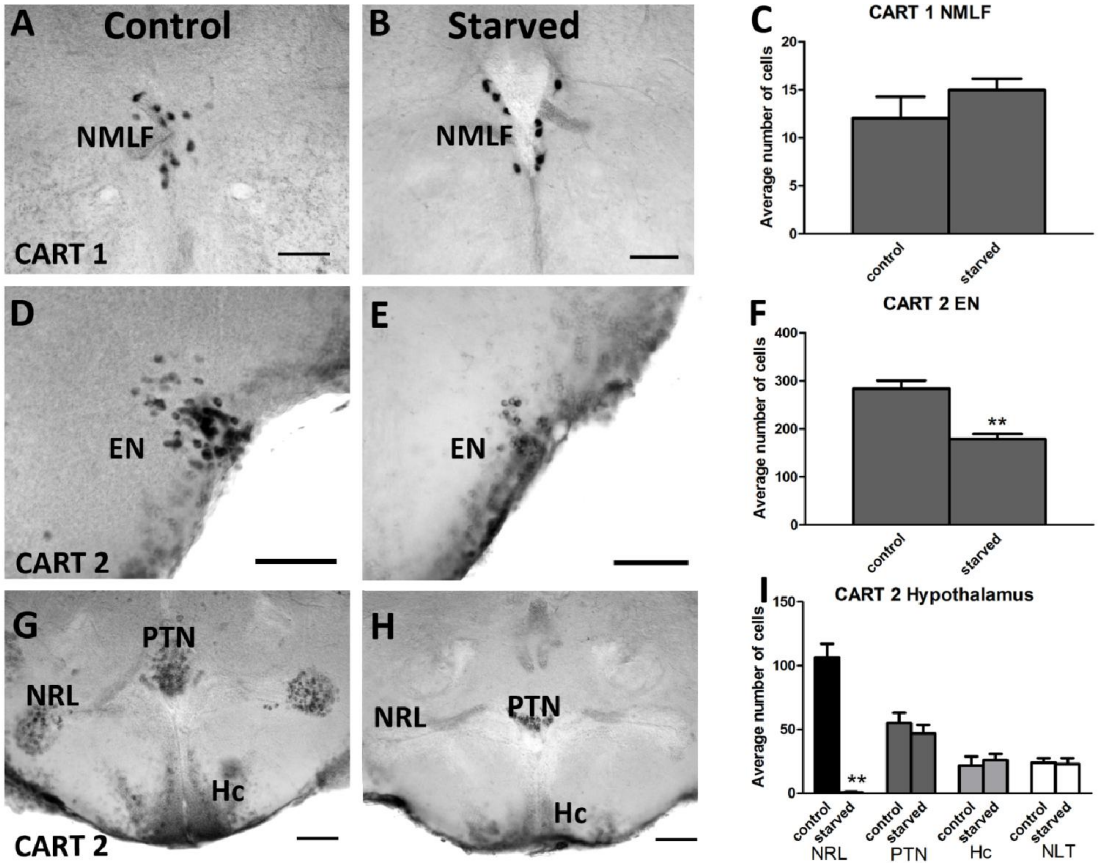

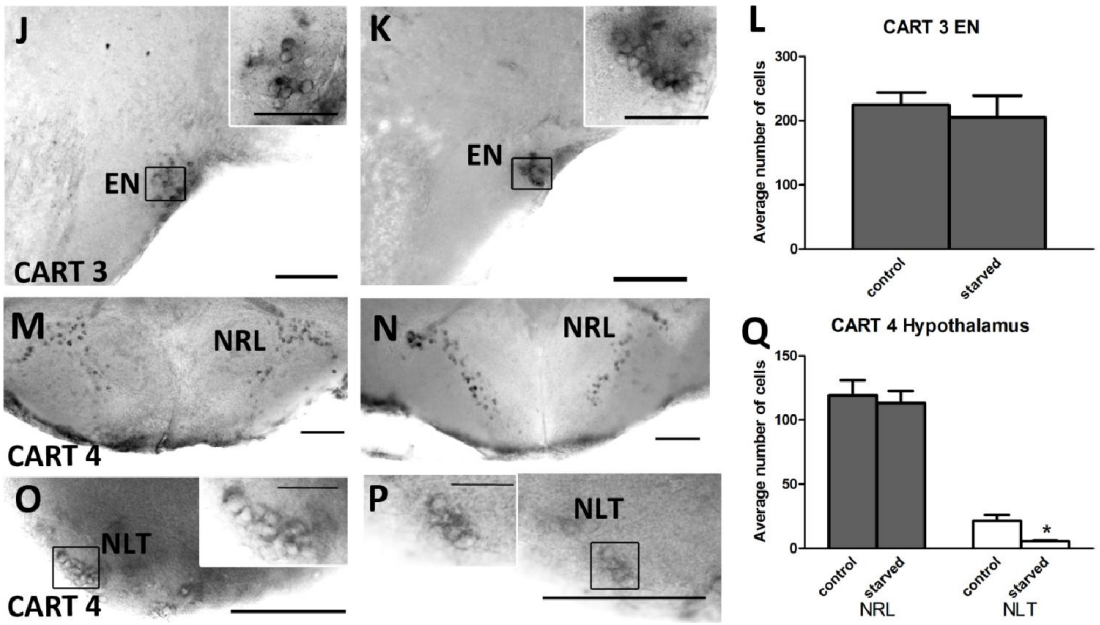

Figure 10: Starvation induced changes in CART gene expression.

Transverse section of the adult female zebrafish brains in the fed control group (**A, D, G, J, M, O**), the starved group (**B, E, H, K, N, P**) and the graphical representation of the cell numbers (**C, F, I, L, Q**). **A – C:** CART 1 containing cells of the NMLF do not respond to starvation; n=5 in each group. **D –F:** CART 2 containing cells of the EN decrease in number upon starvation; n=6. **G – I:** CART 2 expressing neurons of the NRL (n=6) decrease in number following starvation. CART 2 containing cells do not respond to starvation in the PTN (n=5), Hc (n=5) and NLT (n=5). **J – L:** CART 3 expressing EN neurons do not change following starvation; n=6 for each group. **M –Q:** CART 4 expressing NLT neurons decrease in number upon starvation; n=5 in each group. However, the number of CART 4 positive cells in the NRL region does not change upon starvation (n=6). All the cell numbers are Abercrombie corrected averages of CART positive cells in the indicated brain region. Unpaired t-test was used to estimate significance. Error bars indicate mean $\pm$ standard error of mean. * = $p<0.05$, ** = $p<0.005$. Scale bar = 100 µm in **A,B,D,E,G,H,J,K,M,N,O,P**; 25 µm in the insets.

Discussion:

Feeding drive is characterized by initiation of food search and consumption. Since it is necessary for survival, the neural circuits are expected to be hardwired and conserved across species. Zebrafish is an attractive model system to investigate the neural circuits which regulate feeding drive. CART neuropeptide is known to induce anorexia (Kristensen et al., 1998), and is also associated with many other functions such as visual processing, sleep wake behavior, motor control (Subhedar et al., 2014). Zebrafish has 4 known CART genes in its genome (Nishio et al., 2012). In this study we have mapped the distribution of these four CART genes in the whole zebrafish brain using *in situ* hybridization (ISH). CART 1 is expressed only in the NMLF region while CART 3 is expressed only in the EN region. In comparison, CART 2 and CART 4 are widely expressed in the brain, often cohabiting in the same region, which is interesting as CART 2 has highest homology with mammalian CART while CART 4 is most divergent. Such different pattern of expression among the four genes suggests non-redundant functions for the four genes in various circuits.

There are no antibodies which specifically bind to these different CART peptides. Also the affinity of the existing antibody to these different peptides is not characterized. So we used *in situ* hybridization to map the expression pattern. ISH will reveal the perikarya that may not be resolved by immunofluorescence, as the mRNA is likely to localize to the neuronal soma, while the corresponding peptide may be detected in the neurites. Our CART mRNA expression map strongly suggests this notion. For example, in hypothalamus, a major centre for energy homeostasis, only isolated cells were detected using IF (Mukherjee et al., 2012), while our study using ISH reveals multiple groups of CART positive neurons in hypothalamus such as PTN, NRL ,NLT, SCN and Hc. (Nishio et al., 2012) reported CART mRNA distribution in zebrafish larvae, but the less differentiated, developing brain does not offer enough resolution to identify functionally distinct nuclei such as in the hypothalamus of adult zebrafish.

Abundant CART expression in optic tectum, PG, TS, NMLF suggests important role of CART in sensory processing and motor control. Presence of CART in POA and tuberal nuclei indicates CART might be involved in neuroendocrine regulation.

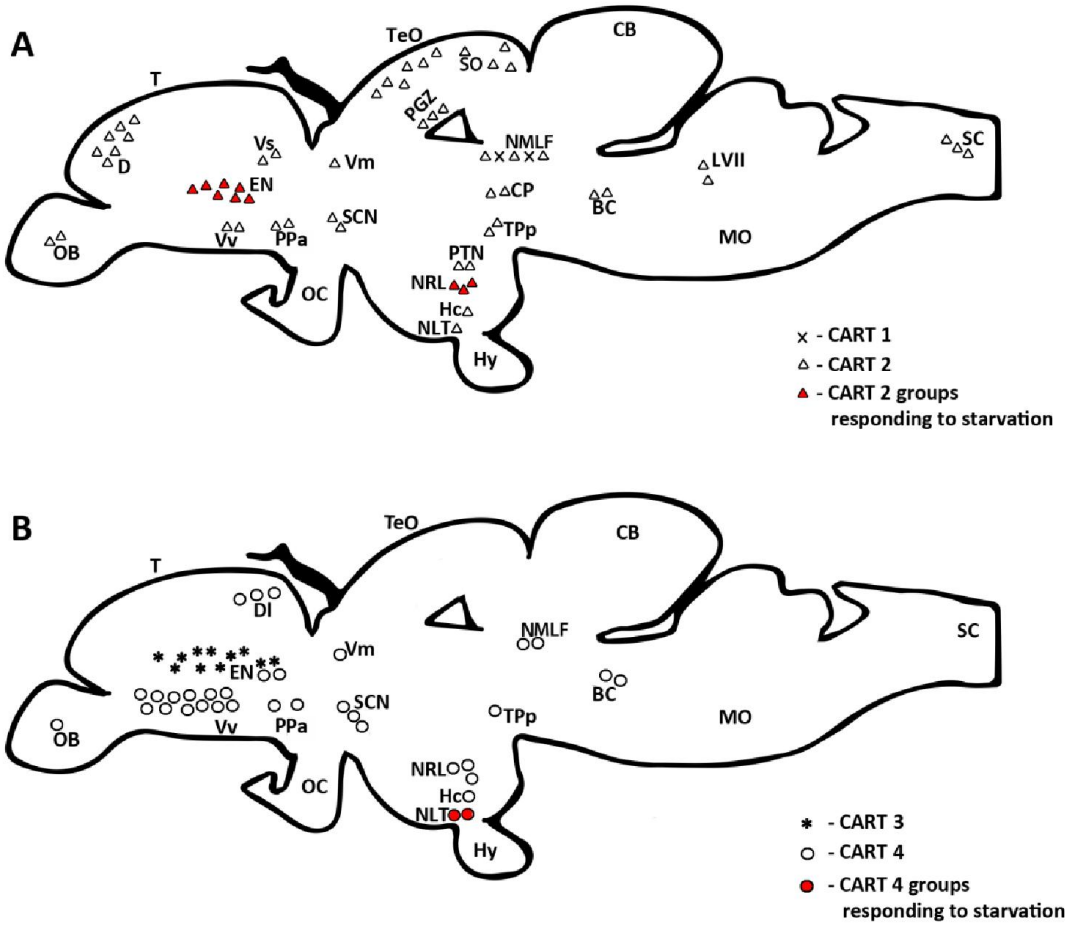

Figure 11: Schematic summary of CART mRNA expression

Schematic lateral view of the adult zebrafish brain showing the distribution of CART 1, CART 2 mRNAs (A) and CART 3, CART 4 mRNAs (B). Neuronal groups responding to starvation are represented by filled symbols.

Olfactory processing

CART is present in the soma and fibers in the olfactory system of the rats (Koylu et al., 1997), especially in abundant amounts in mitral and tufted cells. A sub population of periglomerular cells shows presence of CART and some colocalized with GABA/dopamine (Koylu et al., 1997) suggesting neuromodulation in olfactory processing. CART is also present in glomeruli of the olfactory bulb of catfish (Singru et al., 2007) and frog (Gaupale et al., 2013). Mukherjee et al., 2012 detected CART fibers in glomerular formation of zebrafish using IF. The current study using ISH reveals the presence of CART 2 and CART 4 containing granule cells in in the

internal cell layer of the olfactory bulb. The presence of CART in olfactory system across different phyla suggests that CART has a role in olfactory processing, but functional evidence is still lacking.

Energy homeostasis

Many distinct hypothalamic nuclei in mammals are known to be centers responsible for behaviors regulating energy balance such as paraventricular hypothalamic nuclei and arcuate nucleus. Studies have identified hypothalamic nuclei involved in feeding behavior in teleosts (Copeland et al., 2011). In the present study, starvation led to a significant reduction in the population of CART 2 mRNA expressing neurons of the EN and NRL, and of the CART 4 mRNA expressing cells in the NLT region.

Studies have reported decrease in CART gene expression after fasting in gold fish, catfish and Atlantic salmon (Abbott and Volkoff, 2011; Subhedar et al., 2011; Volkoff et al., 2005). In zebrafish larvae all four CART genes show reduced expression following starvation as determined by quantitative PCR (qPCR) (Nishio et al., 2012). While these PCR based studies report change in expression levels, they are derived from relatively large brain tissue volumes and thus lack spatial resolution to discriminate between different sub-regions of the brain. The current study using ISH provides complementary analysis by identifying regions and gene specific responses to changes in energy status at cellular resolution.

Neuronal populations which respond to changes in energy status

Nucleus lateralis tuberis

The NLT neurons in fish are considered as the equivalent of the arcuate nucleus of rat (Cerdá-Reverter and Peter, 2003). Indeed we find striking similarities between the NLT of teleosts and arcuate nucleus of mammals. As in the rat arcuate nucleus, leptin receptors are expressed in the zebrafish NLT (Copeland et al., 2011; Kristensen et al., 1998). The arcuate nucleus of rat is known to contain POMC/α-MSH as well as CART and play a major role in producing anorexia (Barsh and Schwartz, 2002; Vrang, 2006). `On similar lines, the NLT neurons in zebrafish show POMC and α-MSH expression (Berman et al., 2009; Lohr and Hammerschmidt, 2011). AgRP is yet another major player in the arcuate nucleus of rat, which inhibits

the action of α-MSH and exerts orexigenic affects. In the goldfish, expression of AgRP mRNA was up-regulated after fasting (Cerdá-Reverter and Peter, 2003).Transgenic zebrafish over expressing AgRP exhibit obesity, increased linear growth and adipocyte hypertrophy (Song and Cone, 2007).These convergent observations strongly suggest that, like the arcuate nucleus of rat, the NLT in zebrafish may receive leptin borne adiposity related signal from the periphery and issue output signals mediated by agents like POMC/α-MSH/AgRP/CART which in turn play a key role in orchestrating suitable responses in terms of food intake and energy expenditure.

Nucleus recessus lateralis

NRL neurons show the distinct expression of CART 2 and 4 genes. CART 2 was expressed in the lateral part of lateral recess while CART 4 expressed throughout the recessus. Their responses to change in energy status were also different. CART 2 mRNA expression was completely abolished from the neurons following starvation, while the number of CART 4 mRNA expressing cells did not change. Immunohistochemical analysis show the presence of orexigenic peptide NPY cohabiting in the NRL region where CART 2 is expressed (Kaniganti, 2014), suggesting the role of CART 2 in energy homeostasis. These results underscore the importance of circuit specific investigation of behavior as it suggests non redundant roles for different genes cohabiting in the same region.

Entopeduncular nucleus

The EN is considered analogous to the primate globus pallidus (Amo et al., 2010; Aoki et al., 2013). EN in the telencephanlon emerges as a novel non-hypothalamic center involved in energy homeostasis. Mukherjee et al., 2012 reported CART colocalization with orexigenic peptide NPY in EN neurons using IF and an increase in CART expression with glucose treatment in EN of zebrafish, suggesting a role in energy homeostasis. A comparison of the IF and ISH data suggests that whereas the antibody stained a large population of EN neurons, there is a distinct regional bias regarding the type of CART mRNAs expressed in this region. CART 2 mRNA was mainly detected in the rostral part of the EN, CART 4 was confined to a small subpopulation in the caudal part, and CART 3 was seen throughout the nucleus. Following starvation, a significant reduction in the cell population of CART 2 mRNA

containing cells was observed in the EN region. However, the number of cells expressing CART 3 and CART 4 mRNAs, which are also detected in the EN neurons, did not change following starvation. These differential responses to changes in energy status open up the possibility that the EN may consist of overlapping CART expressing neurons with distinct functional roles.

Yet another point of interest is the likelihood of association of CART with other signaling molecules, which influence feeding behavior. Endocannabinoid signaling is known to influence CART expression in the zebrafish (Nishio et al., 2012). Expression of cannabinoid receptor 1 has been reported close to periventricular regions in the ventral telencephalon (Lam et al., 2006). This region also contains CART 2 mRNA expressing cells. Orexins increased food intake in a wide variety of teleosts (Volkoff et al., 2005). Like CART, orexin containing neurons were detected in the POA, around the lateral recesses and in the hypothalamic tuberal areas of the zebrafish (Kaslin et al., 2004).

Chapter 4

Towards Elucidation of CART Neural Circuitry

We have identified specific CART expressing neuronal populations which respond to changes in energy levels in the zebrafish brain. The next step is to check the role of these neurons by manipulating their activity and investigate the behavioral changes. Such manipulation can be done in many different ways. Electrical stimulation/suppression is generic and will affect all cell types in that region and thus does not offer enough resolution to study individual neuronal circuits. CART gene knockout will affect multiple functions and might inhibit proper development of zebrafish because its expression is seen in the commissural neurons during development (Mukherjee et al., 2012). Since innate purposive behaviors such as feeding are necessary for survival, multiple, parallel and redundant neuronal pathways exist to regulate the feeding behavior (Betley et al., 2013). Knock down or over expression studies might invoke compensatory mechanisms during development to ensure survival. Thus it is necessary to manipulate the activity of neurons in a temporally and spatially precise manner. Zebrafish larva is a promising model system to study neural circuits because it is transparent and thus optically accessible to do precise neuronal manipulations. Two key tools which are necessary to do circuit manipulation studies are transgenic zebrafish expressing molecular tools specific to neuronal populations of interest to do precise manipulations and a behavioral assay to quantify the feeding behavior. To that end we are generating transgenic zebrafish by cloning the promoter regions of CART 2 and 4 and we have developed a high throughput feeding assay to quantify the food intake by zebrafish larvae.

Materials and Methods

Preparation of fluorescently labeled paramecia:

The feeding assay employed in this study is according to (Shimada et al., 2012). Paramecia were cultured in a medium consisting of 0.5 g/l of dry yeast and 4-5 boiled wheat grains in distilled water. At the appropriate density, paramecia were collected using light in a shaded bottle, and then filtered through a coarse mesh (200 µm) and a fine mesh (40 µm) filter. The filtered paramecia were concentrated by centrifuging 50 ml of the culture at 4000 rpm for 5 min and resuspending them in 5 ml of distilled water. The paramecia were quantified by measuring optical density at 600 nm using biophotometer (Eppendorf, Hamburg,Germany). For fluorescent labeling of the paramecia, CellTracker™-CM DiI (Life Technologies, Carlsbad, CA) was used. 1 µg of CM DiI was added to the paramecia and were stained for 1 hr. The residual dye was removed by centrifuging and washing the paramecia.

Quantification of paramecia intake

Fluorescently labeled paramecia were fed to 7 dpf larvae. 10 larvae were transferred to 6 well plate containing 3 ml of E3 medium and 10000 fluorescently labeled paramecia were added. In glucose treatment group the larvae were allowed to feed on paramecia in E3 medium consisting of 2% glucose. The larvae were allowed to feed for 1 and 3 hrs after which they were washed and kept one in each well of round bottom white 96 well plate (Thermo Scientific, MA) containing anesthesia (1:2000; 2-phenoxy ethanol). The fluorescent signal was measured using Tecan infinite M200 pro plate reader in well scan mode with 5 repeats using a fluorescent filter set (excitation wavelength - 545 nm, emission wavelength – 575 nm). The fluorescence intensity was defined to be proportional to the amount of paramecia fed to each zebrafish.

Results

Feeding behavior of zebrafish larvae were assayed using fluorescently labeled paramecia. The protocol is summarized in the figure 12A. The number of paramecia in distilled water corresponds to the optical density at 600nm (Fig. 12C, with Aditi

Maduskar). Paramecia stained using the lipophilic dye CM DiI showed normal motility. Zebrafish fed with labeled paramecia showed fluorescence in the abdominal region, while the zebrafish which were fed with unlabeled paramecia did not show any fluorescence (Fig.12B). The fluorescent intensity of glucose treated zebrafish was significantly lower than control zebrafish ($P<0.05$, Fig.12D).

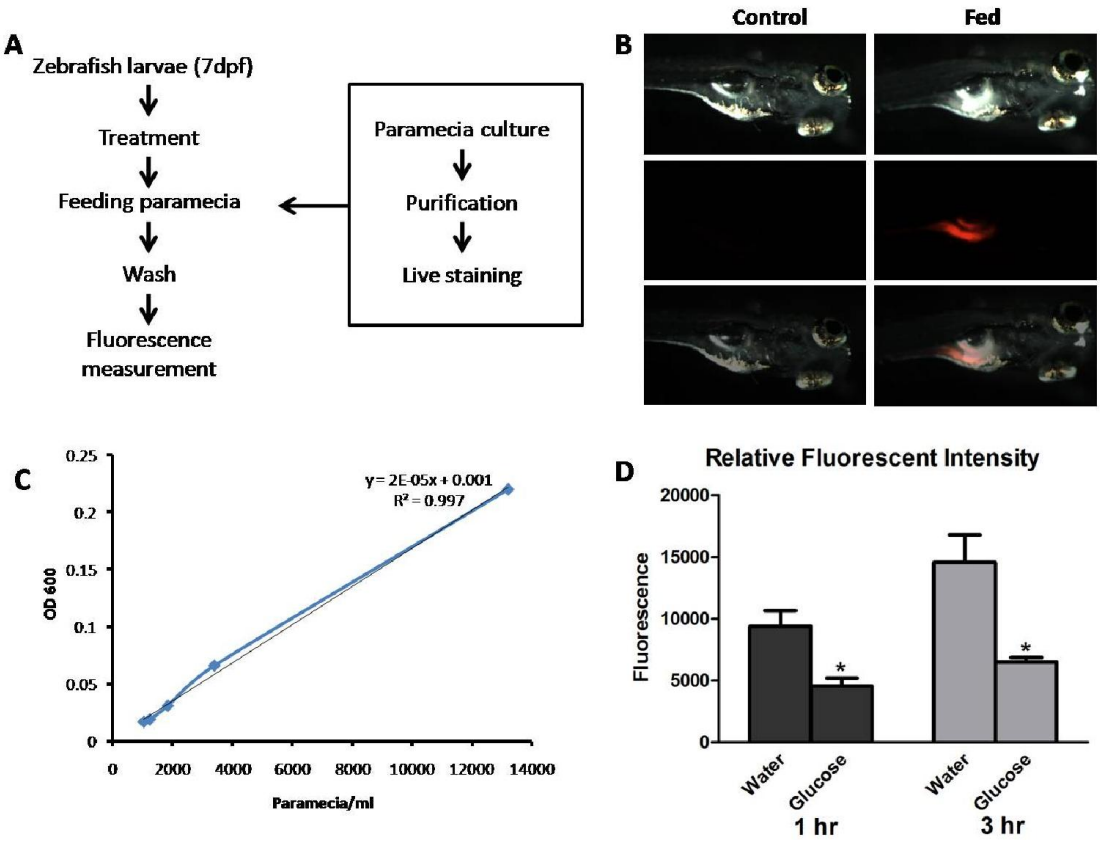

Figure 12: Larval Feeding assay

A: Schematic representation of the protocol followed for the larval feeding assay. **B:** Larvae fed with fluorescent paramecia shows fluorescence while the control does not show any fluorescence. Brightfield, fluorescence and overlay image is shown **C:** The actual numbers of paramecia correlated with optical density at 600nm (OD 600). **D:** Fluorescent intensities of larvae fed with labeled paramecia in water and in water containing glucose for 1hr and 3hrs. * indicates $P<0.05$. (control, water 1 hr and 3 hr n=8, glucose 1 hr n=5, glucose 3 hr n=7) Error bars indicate mean $\pm$ standard error of mean.

Discussion

Zebrafish exhibits a large variety of behaviors such as scototaxis, thigmotaxis, social interaction, novel tank diving test, bouncing ball assay which makes it a good model

system to functionally characterize neural circuits of behavior (Kalueff et al., 2013). In this study, we developed and optimized a high throughput behavioral assay to quantify feeding in zebrafish larvae. Current feeding behavioral assays in adult zebrafish involves manual counting of number of food pellets consumed (Yokobori et al., 2012) or monitoring number of biting attempts (Wakhloo et al., unpublished work) or measuring *Artemia* numbers. But the feasibility of neural circuit manipulations in adult zebrafish is limited, while zebrafish larva is well suited for acute specific circuit manipulations owing to its small and optically transparent body. This makes it imperative to develop behavioral assays to utilize the full potential of zebrafish larvae. Existing feeding behavior assays in larvae measures number of paramecia consumed or analyze prey capture maneuvers (Gahtan et al., 2005). These techniques require sophisticated instrument such as a high frame rate camera or they involve complex analysis. We have optimized a feeding assay (Shimada et al., 2012) which is high throughput and directly measures the amount of food intake using fluorescence as readout. We have validated this assay by testing it with glucose treatment. Glucose treatment should mimic satiety and thus should decrease food intake. This is evident in the figure 12D. The larvae treated with glucose show significantly lower fluorescence compared to the control larvae suggesting reduced feeding in glucose treated group. This is a proof of principle for the validity of the behavioral assay, but the assay needs to be further standardized. The optimum feeding time, optimum paramecia concentration for feeding needs to be determined. This assay can be used as a behavioral readout, when specific nodes of the CART neural circuit are manipulated.

Chapter 5

Energy Status Dependant Modulation of Olfactory Sensitivity

Sensory sensitivity is modulated during energy deficit conditions to increase the drive to consume food and counteract the deficit. However the neural mechanism behind this process is not clear. Neuropeptide Y is an orexigenic peptide which increases food intake in zebrafish when administered through icv route (Yokobori et al., 2012). NPY has been reported to occur in different parts of olfactory system across vertebrate phyla. NPY immunoreactivity was seen in terminal nerve of axolotl (Mousley et al., 2006), in olfactory receptor neurons and olfactory bulb in catfish (Gaikwad et al., 2004) and in olfactory bulb of gold fish (Peng et al., 1994)

In zebrafish, intense NPY expression was seen in the olfactory bulb and in the olfactory organ especially in the olfactory sensory neurons (Deogade, 2012). Behavioral studies by Deogade (unpublished work) showed that NPY is involved in perception of amino acids in zebrafish. Zebrafish spend more time in the part of the tank where amino acid were being delivered while the time spent was reduced when BIBP – a NPY receptor inhibitor was administered suggesting that NPY might mediate a role in amino acid perception. Since NPY being a strong orexigenic peptide in zebrafish (Yokobori et al., 2012), we hypothesize that NPY might modulate olfactory sensitivity in the olfactory epithelia. Immunohistochemical studies show that NPY expression in the olfactory epithelia decrease on glucose administration and increase upon starvation (Kaniganti, 2014). We have developed and optimized electro-olfactogram to functionally understand, if the gain of olfactory sensitivity is modified upon changes in energy status and if NPY has a role in modulating the olfactory gain.

Materials and Methods

Electro-olfactogram (EOG)

The EOG setup built here was adapted from (Michel et al., 2003). Zebrafish was anesthetized in 2-phenoxy ethanol and kept covered in a moist paper towel in a

custom built recording chamber (Fig. 13C,D). Anesthesia was delivered using a soft tube inserted in the mouth and the rate of delivery was regulated using gravity flow (Fig. 13B,E). EOG is the sum of receptor potential of olfactory receptor neurons and thus producing a characteristic slow negative change in DC voltage potential. To record these responses, a stainless steel recording electrode (Fig. 13A) was placed on one of the olfactory epithelium. A ground wire was placed beneath the body of the fish. A constant flow of water to the olfactory epithelium was maintained using gravity flow. The responses were filtered at 0.1 Hz - 0.1 KHz and amplified using low noise DAM 70 differential amplifier (World Precision Instruments, FL). The signals were then acquired using a NI 6008 (National Instruments, TX) data acquisition card (DAQ) controlled by NI signal express software in a computer (Fig. 13B).

Odorant delivery

To mimic food related odorants, a mixture of 8 amino acids was prepared. It consisted of lysine, valine, L cysteine, methionine, alanine, phenylalanine, histidine, tryptophan. A 250µl bolus of odorant was directly injected into the constant gravity flow of water to the olfactory epithelium to avoid artifacts due to physical disruptions (Fig. 13B). Different odorant concentrations were delivered and the responses were studied to test for the validity of the setup.

Glucose treatment

Adult zebrafish were anesthetized with 2-phenoxy ethanol (1:2000) and intracerebroventricularly (icv) injected with 8000ng of glucose in the glucose group and saline in the starved group (starved for 6 days) using a Hamilton microsyringe.

Data analysis

The EOG traces were filtered to reduce noise, corrected for zero offset and the negative peak amplitude was measured to get the magnitude of response. In the concentration response curve, three EOG traces obtained from a single fish were averaged and were represented with standard error mean. In glucose-starved fish experiment, 11 (glucose) and 15 (starved) traces obtained from two fishes were averaged and represented with standard error mean.

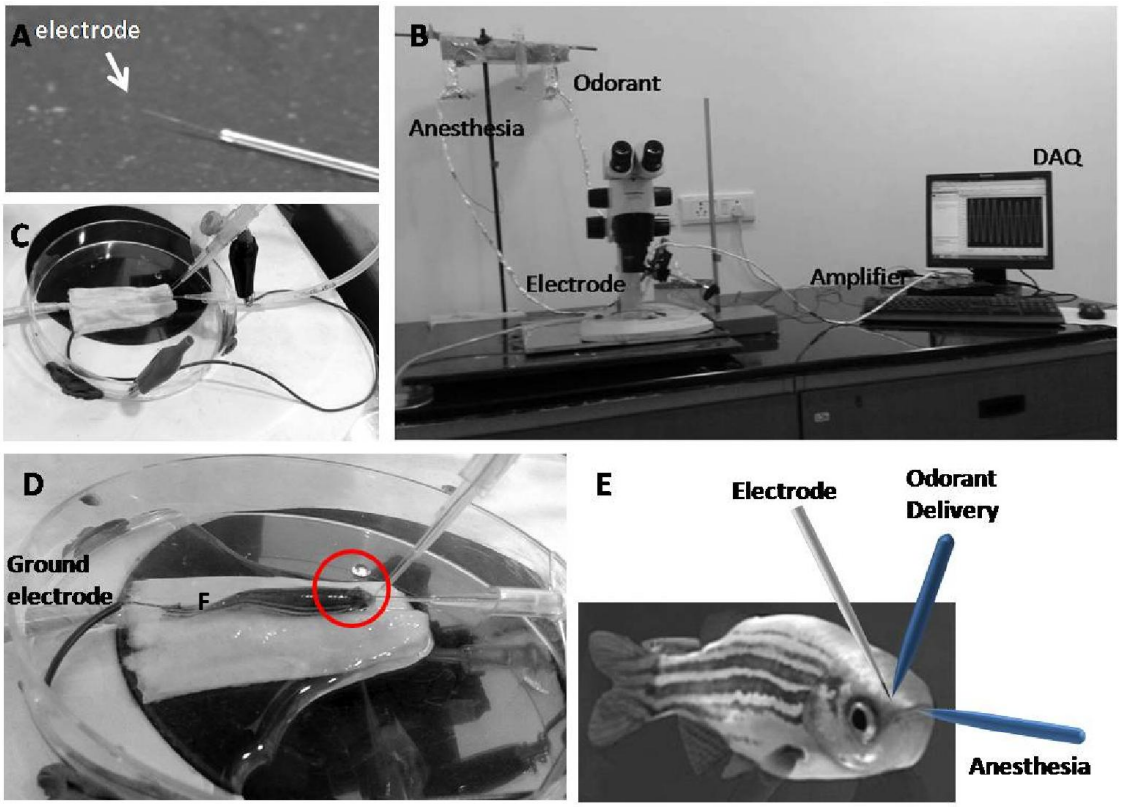

Figure 13: EOG experimental setup

A: fabricated electrode **B:** whole experimental setup showing gravity flow system, recording chamber, amplifier and data acquisition **C:** custom built chamber for recording EOG **D:** recording in an anesthetized fish with perfusion. **E:** position of electrode, anesthesia and odorant delivery tube in the fish.

Results and Discussion

Electro-olfactogram setup was built and standardized to measure average neuronal activity in the olfactory epithelium of zebrafish. The setup was validated by measuring the EOG response magnitude with varying odor concentration. The amplitude of EOG response increases with increase in odor concentration (100μM, 500μM, 1mM, 100mM, Fig. 14A). Preliminary results from experiments suggest that the ensemble activity of the olfactory sensory neurons in the olfactory epithelium is modulated based on energy levels. The magnitude of EOG response in the glucose group was significantly lower than the starved group suggesting that the olfactory

gain increases upon decrease in energy levels. Even though this experiment shows the trend in the change in response with respect to energy status, biological replicates are necessary to get statistically significant results.

There are many studies on *C. elegans* (Colbert and Bargmann, 1997), axoltols (Mousley et al., 2006) and on rodents (Negroni et al., 2012) investigating the relation between feeding and modulation of sensory sensitivity, but the neural circuitry underlying this modulation of sensory sensitivity starting from interoceptors and role of different neuromodulators is poorly understood. Here we developed EOG setup to functionally determine the change in olfactory gain. Electrical activity data along with behavioral and anatomical studies (Deogade, 2012; Kaniganti, 2014) will provide an elaborate picture of how NPY might modulate olfactory sensitivity.

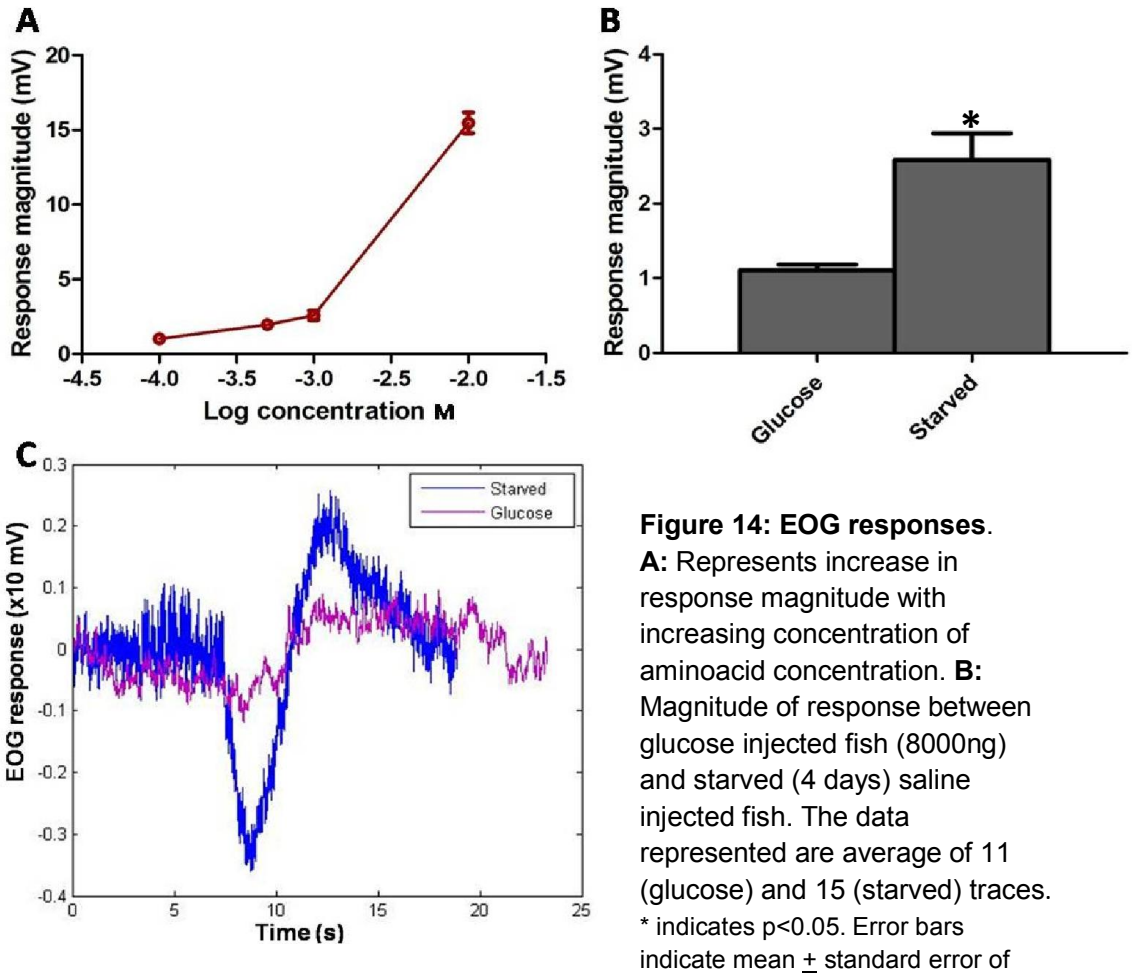

Figure 14: EOG responses. **A:** Represents increase in response magnitude with increasing concentration of aminoacid concentration. **B:** Magnitude of response between glucose injected fish (8000ng) and starved (4 days) saline injected fish. The data represented are average of 11 (glucose) and 15 (starved) traces. * indicates $p<0.05$. Error bars indicate mean $\pm$ standard error of mean.

Chapter 6

Conclusion

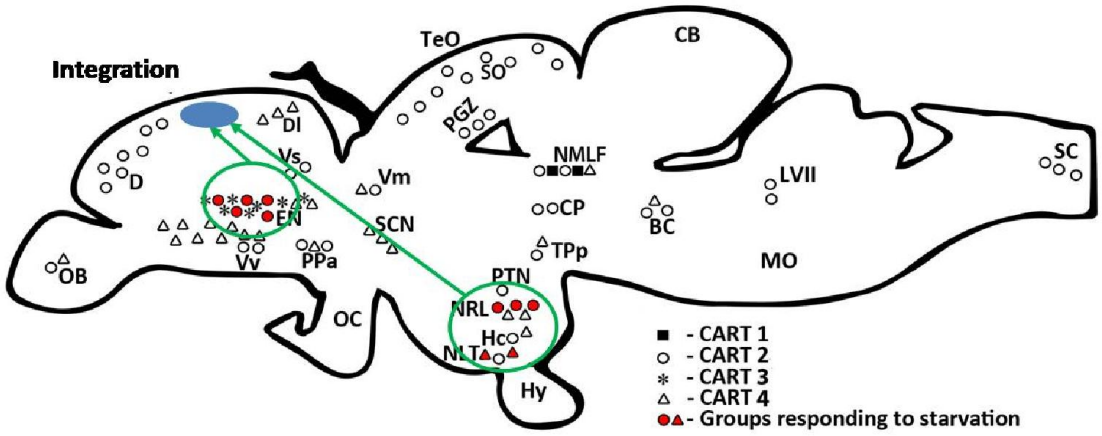

Figure 15: CART neural circuitry in regulating feeding drive

Behaviors such as feeding or not feeding are relatively long lasting behavior compared to the neuronal activity, and how this short term neuronal activity translates into maintaining sustained behavioral states is not understood. One possible mechanism is that the short term electrical activity is converted into biochemical activity by the action of neuromodulators which have longer time scales. CART is a potent neuromodulator and induces anorexia. The expression pattern of the four CART mRNAs in the adult zebrafish brain has been mapped and it generally agrees with the expression of the peptide (Mukherjee et al., 2012). Further genetically defined neuronal populations in the hypothalamus and telencephalon which respond to changes in energy status have been identified. The CART 2 and CART 4 neurons in NRL, NLT, and EN might be the key neurons which respond to internal state change and may have a role in inducing anorexia. Neurons from these multiple nuclei project to dorsomedial telencephalon (Kaniganti, 2014) where Wakhloo et al. (unpublished work) detected ERK activity upon administration of CART. When this ERK activation is blocked, the CART induced anorexia is abolished (Wakhloo et al., unpublished work). These suggest that the information from disparate CART nuclei might be integrated in the dorsal telencephalon to

produce a behavioral state switch. The processing involved in these circuits can be understood by acute manipulation of those neurons in a behaving animal.

Zebrafish larva is a promising model system to perform precise and acute neuronal manipulations using light because of its optical transparency. One can create transgenic zebrafish expressing different opsins (light sensitive ion channels) to modify the activity of specific neurons. To that end we are developing transgenic gene constructs and have developed a high throughput behavioral assay to quantify feeding behavior in zebrafish larvae, which will be used as a behavioral readout during circuit manipulations.

We have developed and optimized electro-olfactogram for investigation of the modulation of olfactory sensitivity with changes in energy levels. Preliminary EOG data suggest that olfactory sensitivity in energy deficit fish is high compared to sated fish. We plan to compare the EOG responses by administering exogenous NPY and BIBP (NPY receptor blocker) in starved and sated fish to dissect out the role of NPY in the centrifugal modulation of olfactory sensitivity.

References

1. Abbott, C.R., Rossi, M., Wren, A.M., Murphy, K.G., Kennedy, A.R., Stanley, S.A., Zollner, A.N., Morgan, D.G., Morgan, I., Ghatei, M.A*., et al.* (2001). Evidence of an orexigenic role for cocaine- and amphetamine-regulated transcript after administration into discrete hypothalamic nuclei. Endocrinology *142*, 3457-3463.
2. Abbott, M., and Volkoff, H. (2011). Thyrotropin Releasing Hormone (TRH) in goldfish *(Carassius auratus)*: role in the regulation of feeding and locomotor behaviors and interactions with the orexin system and cocaine- and amphetamine regulated transcript (CART). Horm Behav *59*, 236-245.
3. Abercrombie, M. (1946). Estimation of nuclear population from microtome sections. Anat Rec *94*, 239-247.
4. Amo, R., Aizawa, H., Takahoko, M., Kobayashi, M., Takahashi, R., Aoki, T., and Okamoto, H. (2010). Identification of the zebrafish ventral habenula as a homolog of the mammalian lateral habenula. J Neurosci *30*, 1566-1574.
5. Aoki, T., Kinoshita, M., Aoki, R., Agetsuma, M., Aizawa, H., Yamazaki, M., Takahoko, M., Amo, R., Arata, A., Higashijima, S*., et al.* (2013). Imaging of neural ensemble for the retrieval of a learned behavioral program. Neuron *78*, 881-894.
6. Barsh, G.S., and Schwartz, M.W. (2002). Genetic approaches to studying energy balance: perception and integration. Nat Rev Genet *3*, 589-600.
7. Berman, J.R., Skariah, G., Maro, G.S., Mignot, E., and Mourrain, P. (2009). Characterization of two melanin-concentrating hormone genes in zebrafish reveals evolutionary and physiological links with the mammalian MCH system. J Comp Neurol *517*, 695-710.
8. Betley, J.N., Cao, Z.F., Ritola, K.D., and Sternson, S.M. (2013). Parallel, redundant circuit organization for homeostatic control of feeding behavior. Cell *155*, 1337-1350.
9. Castro, A., Becerra, M., Manso, M.J., Tello, J., Sherwood, N.M., and Anadón, R. (2009). Distribution of growth hormone-releasing hormone-like peptide: Immunoreactivity in the central nervous system of the adult zebrafish *(Danio rerio)*. J Comp Neurol *513*, 685-701.
10. Cerdá-Reverter, J.M., and Peter, R.E. (2003). Endogenous melanocortin antagonist in fish: structure, brain mapping, and regulation by fasting of the goldfish agouti-related protein gene. Endocrinology *144*, 4552-4561.
11. Colbert, H.A., and Bargmann, C.I. (1997). Environmental signals modulate olfactory acuity, discrimination, and memory in *Caenorhabditis elegans*. Learning & memory *4*, 179-191.
12. Conde-Sieira, M., Agulleiro, M.J., Aguilar, A.J., Miguez, J.M., Cerda-Reverter, J.M., and Soengas, J.L. (2010). Effect of different glycaemic conditions on gene expression of neuropeptides involved in control of food intake in rainbow trout; interaction with stress. J Exp Biol *213*, 3858-3865.
13. Copeland, D.L., Duff, R.J., Liu, Q., Prokop, J., and Londraville, R.L. (2011). Leptin in teleost fishes: an argument for comparative study. Front Physiol *2*, 26.
14. Dandekar, M.P., Singru, P.S., Kokare, D.M., and Subhedar, N.K. (2009). Cocaine- and amphetamine-regulated transcript peptide plays a role in the manifestation of depression: social isolation and olfactory bulbectomy models reveal unifying principles. Neuropsychopharmacology *34*, 1288-1300.
15. Deogade, A. (2012). Neuropeptide Y: A Novel Olfactory Modulator in Zebrafish, Danio Rerio (IISER Pune).
16. Douglass, J., McKinzie, A.A., and Couceyro, P. (1995). PCR differential display identifies a rat brain mRNA that is transcriptionally regulated by cocaine and amphetamine. J Neurosci *15*, 2471-2481.
17. English, J.D., and Sweatt, J.D. (1996). Activation of p42 mitogen-activated protein kinase in hippocampal long term potentiation. The Journal of biological chemistry *271*, 24329-24332.

18. Gahtan, E., Tanger, P., and Baier, H. (2005). Visual prey capture in larval zebrafish is controlled by identified reticulospinal neurons downstream of the tectum. J Neurosci *25*, 9294-9303.
19. Gaikwad, A., Biju, K.C., Saha, S.G., and Subhedar, N. (2004). Neuropeptide Y in the olfactory system, forebrain and pituitary of the teleost, *Clarias batrachus*. J Chem Neuroanat *27*, 55-70.
20. Gaupale, T.C., Subhedar, N., and Bhargava, S. (2013). Ontogeny of cocaine- and amphetamine-regulated transcript peptide in brain of frog, *Microhyla ornata*. Gen Comp Endocrinol *181*, 77-87.
21. Gautvik, K.M., de Lecea, L., Gautvik, V.T., Danielson, P.E., Tranque, P., Dopazo, A., Bloom, F.E., and Sutcliffe, J.G. (1996). Overview of the most prevalent hypothalamus-specific mRNAs, as identified by directional tag PCR subtraction. Proc Natl Acad Sci U S A *93*, 8733-8738.
22. Germano, C.M., de Castro, M., Rorato, R., Laguna, M.T., Antunes-Rodrigues, J., Elias, C.F., and Elias, L.L. (2007). Time course effects of adrenalectomy and food intake on cocaine- and amphetamine-regulated transcript expression in the hypothalamus. Brain Res *1166*, 55-64.
23. Hubert, G.W., Jones, D.C., Moffett, M.C., Rogge, G., and Kuhar, M.J. (2008). CART peptides as modulators of dopamine and psychostimulants and interactions with the mesolimbic dopaminergic system. Biochem Pharmacol *75*, 57-62.
24. Inagaki, H.K., Ben-Tabou de-Leon, S., Wong, A.M., Jagadish, S., Ishimoto, H., Barnea, G., Kitamoto, T., Axel, R., and Anderson, D.J. (2012). Visualizing neuromodulation in vivo: TANGO-mapping of dopamine signaling reveals appetite control of sugar sensing. Cell *148*, 583-595.
25. Kalueff, A.V., Gebhardt, M., Stewart, A.M., Cachat, J.M., Brimmer, M., Chawla, J.S., Craddock, C., Kyzar, E.J., Roth, A., Landsman, S.*, et al.* (2013). Towards a comprehensive catalog of zebrafish behavior 1.0 and beyond. Zebrafish *10*, 70-86.
26. Kaniganti, T. (2014). Neural mechanisms underlying feeding drive (IISER Pune).
27. Kaslin, J., Nystedt, J.M., Ostergard, M., Peitsaro, N., and Panula, P. (2004). The orexin/hypocretin system in zebrafish is connected to the aminergic and cholinergic systems. J Neurosci *24*, 2678-2689.
28. Kimmel, H.L., Gong, W., Vechia, S.D., Hunter, R.G., and Kuhar, M.J. (2000). Intra-ventral tegmental area injection of rat cocaine and amphetamine-regulated transcript peptide 55-102 induces locomotor activity and promotes conditioned place preference. J Pharmacol Exp Ther *294*, 784-792.
29. Koylu, E.O., Couceyro, P.R., Lambert, P.D., and Kuhar, M.J. (1998). Cocaine- and amphetamine-regulated transcript peptide immunohistochemical localization in the rat brain. J Comp Neurol *391*, 115-132.
30. Koylu, E.O., Couceyro, P.R., Lambert, P.D., Ling, N.C., DeSouza, E.B., and Kuhar, M.J. (1997). Immunohistochemical localization of novel CART peptides in rat hypothalamus, pituitary and adrenal gland. J Neuroendocrinol *9*, 823-833.
31. Kristensen, P., Judge, M.E., Thim, L., Ribel, U., Christjansen, K.N., Wulff, B.S., Clausen, J.T., Jensen, P.B., Madsen, O.D., Vrang, N.*, et al.* (1998). Hypothalamic CART is a new anorectic peptide regulated by leptin. Nature *393*, 72-76.
32. Kuhn, E., and Koster, R.W. (2010). Analysis of gene expression by in situ hybridization on adult zebrafish brain sections. Cold Spring Harb Protoc *2010*, pdb prot5382.
33. Lam, C.S., Rastegar, S., and Strahle, U. (2006). Distribution of cannabinoid receptor 1 in the CNS of zebrafish. Neuroscience *138*, 83-95.
34. Lohr, H., and Hammerschmidt, M. (2011). Zebrafish in endocrine systems: recent advances and implications for human disease. Annu Rev Physiol *73*, 183-211.

35. Michel, W.C., Sanderson, M.J., Olson, J.K., and Lipschitz, D.L. (2003). Evidence of a novel transduction pathway mediating detection of polyamines by the zebrafish olfactory system. J Exp Biol *206*, 1697-1706.
36. Mousley, A., Polese, G., Marks, N.J., and Eisthen, H.L. (2006). Terminal nerve-derived neuropeptide y modulates physiological responses in the olfactory epithelium of hungry axolotls (*Ambystoma mexicanum*). J Neurosci *26*, 7707-7717.
37. Mueller, T., and Wullimann, M.F. (2005). Atlas of early zebrafish brain development: a tool for molecular neurogenetics (Amsterdam: Elsevier).
38. Mukherjee, A., Subhedar, N.K., and Ghose, A. (2012). Ontogeny of the cocaine- and amphetamine-regulated transcript (CART) neuropeptide system in the brain of zebrafish, Danio rerio. J Comp Neurol *520*, 770-797.
39. Murashita, K., and Kurokawa, T. (2011). Multiple cocaine- and amphetamine-regulated transcript (CART) genes in medaka, *Oryzias latipes*: cloning, tissue distribution and effect of starvation. Gen Comp Endocrinol *170*, 494-500.
40. Negroni, J., Meunier, N., Monnerie, R., Salesse, R., Baly, C., Caillol, M., and Congar, P. (2012). Neuropeptide Y enhances olfactory mucosa responses to odorant in hungry rats. PloS one *7*, e45266.
41. Nishio, S., Gibert, Y., Berekelya, L., Bernard, L., Brunet, F., Guillot, E., Le Bail, J.C., Sanchez, J.A., Galzin, A.M., Triqueneaux, G.*, et al.* (2012). Fasting induces CART down-regulation in the zebrafish nervous system in a cannabinoid receptor 1-dependent manner. Mol Endocrinol *26*, 1316-1326.
42. Peng, C., Gallin, W., Peter, R.E., Blomqvist, A.G., and Larhammar, D. (1994). Neuropeptide-Y gene expression in the goldfish brain: distribution and regulation by ovarian steroids. Endocrinology *134*, 1095-1103.
43. Portugues, R., Severi, K.E., Wyart, C., and Ahrens, M.B. (2013). Optogenetics in a transparent animal: circuit function in the larval zebrafish. Current opinion in neurobiology *23*, 119-126.
44. Root, C.M., Ko, K.I., Jafari, A., and Wang, J.W. (2011). Presynaptic facilitation by neuropeptide signaling mediates odor-driven food search. Cell *145*, 133-144.
45. Shimada, Y., Hirano, M., Nishimura, Y., and Tanaka, T. (2012). A high-throughput fluorescence-based assay system for appetite-regulating gene and drug screening. PloS one *7*, e52549.
46. Singru, P.S., Mazumdar, M., Sakharkar, A.J., Lechan, R.M., Thim, L., Clausen, J.T., and Subhedar, N.K. (2007). Immunohistochemical localization of cocaine- and amphetamine-regulated transcript peptide in the brain of the catfish, *Clarias batrachus* (Linn.). J Comp Neurol *502*, 215-235.
47. Smith, K.L., Gardiner, J.V., Ward, H.L., Kong, W.M., Murphy, K.G., Martin, N.M., Ghatei, M.A., and Bloom, S.R. (2008). Overexpression of CART in the PVN increases food intake and weight gain in rats. Obesity *16*, 2239-2244.
48. Song, Y., and Cone, R.D. (2007). Creation of a genetic model of obesity in a teleost. FASEB journal : official publication of the Federation of American Societies for Experimental Biology *21*, 2042-2049.
49. Subhedar, N., Barsagade, V.G., Singru, P.S., Thim, L., and Clausen, J.T. (2011). Cocaine- and amphetamine-regulated transcript peptide (CART) in the telencephalon of the catfish, *Clarias gariepinus*: distribution and response to fasting, 2-deoxy-D-glucose, glucose, insulin, and leptin treatments. J Comp Neurol *519*, 1281-1300.
50. Subhedar, N.K., Nakhate, K.T., Upadhya, M.A., and Kokare, D.M. (2014). CART in the brain of vertebrates: Circuits, functions and evolution. Peptides *54C*, 108-130.
51. Upadhya, M.A., Dandekar, M.P., Kokare, D.M., Singru, P.S., and Subhedar, N.K. (2011a). Evidence for the participation of cocaine- and amphetamine-regulated transcript peptide (CART) in the fluoxetine-induced anti-hyperalgesia in neuropathic rats. Peptides *32*, 317-326.

52. Upadhya, M.A., Nakhate, K.T., Kokare, D.M., Singru, P.S., and Subhedar, N.K. (2011b). Cocaine- and amphetamine-regulated transcript peptide increases spatial learning and memory in rats. Life Sci *88*, 322-334.
53. Volkoff, H., Canosa, L.F., Unniappan, S., Cerda-Reverter, J.M., Bernier, N.J., Kelly, S.P., and Peter, R.E. (2005). Neuropeptides and the control of food intake in fish. Gen Comp Endocrinol *142*, 3-19.
54. Volkoff, H., and Peter, R.E. (2000). Effects of CART peptides on food consumption, feeding and associated behaviors in the goldfish, *Carassius auratus*: actions on neuropeptide Y- and orexin A-induced feeding. Brain Res *887*, 125-133.
55. Volkoff, H., and Peter, R.E. (2001). Characterization of two forms of cocaine- and amphetamine-regulated transcript (CART) peptide precursors in goldfish: molecular cloning and distribution, modulation of expression by nutritional status, and interactions with leptin. Endocrinology *142*, 5076-5088.
56. Vrang, N. (2006). Anatomy of hypothalamic CART neurons. Peptides *27*, 1970-1980.
57. Vrang, N., Kristensen, P., Tang-Christensen, M., and Larsen, P.J. (2002). Effects of leptin on arcuate pro-opiomelanocortin and cocaine-amphetamine-regulated transcript expression are independent of circulating levels of corticosterone. J Neuroendocrinol *14*, 880-886.
58. Vrang, N., Larsen, P.J., Kristensen, P., and Tang-Christensen, M. (2000). Central administration of cocaine-amphetamine-regulated transcript activates hypothalamic neuroendocrine neurons in the rat. Endocrinology *141*, 794-801.
59. Wullimann, M.F., Rupp, B., and Reichert, H. (1996). Neuroanatomy of the zebrafish brain: a topological atlas. (Basel: Birkhauser Verlag.).
60. Yokobori, E., Azuma, M., Nishiguchi, R., Kang, K.S., Kamijo, M., Uchiyama, M., and Matsuda, K. (2012). Neuropeptide Y stimulates food intake in the Zebrafish, *Danio rerio*. J Neuroendocrinol *24*, 766-773.